Swansea University
Prifysgol Abertawe

Cronfa
Setting Research Free

Cronfa - Swansea University Open Access Repository

This is an author produced version of a paper published in:
IEEE Transactions on Geoscience and Remote Sensing

Cronfa URL for this paper:
http://cronfa.swan.ac.uk/Record/cronfa38335

Paper:
Ledger, P. & Lionheart, W. An Explicit Formula for the Magnetic Polarizability Tensor for Object Characterisation. *IEEE Transactions on Geoscience and Remote Sensing*(99), 1-14.
http://dx.doi.org/10.1109/TGRS.2018. 2801359

Distributed under the terms of a Creative Commons Attribution CC-BY 3.0 License.

This item is brought to you by Swansea University. Any person downloading material is agreeing to abide by the terms of the repository licence. Copies of full text items may be used or reproduced in any format or medium, without prior permission for personal research or study, educational or non-commercial purposes only. The copyright for any work remains with the original author unless otherwise specified. The full-text must not be sold in any format or medium without the formal permission of the copyright holder.

Permission for multiple reproductions should be obtained from the original author.

Authors are personally responsible for adhering to copyright and publisher restrictions when uploading content to the repository.

http://www.swansea.ac.uk/library/researchsupport/ris-support/

This article has been accepted for inclusion in a future issue of this journal. Content is final as presented, with the exception of pagination.

An Explicit Formula for the Magnetic Polarizability Tensor for Object Characterization

Paul D. Ledger and William R. B. Lionheart

***Abstract*— The magnetic polarizability tensor (MPT) has attracted considerable interest due to the possibility it offers for characterizing conducting objects and assisting with the identification and location of hidden targets in metal detection. An explicit formula for its calculation for arbitrary-shaped objects is missing in the electrical engineering literature. Furthermore, the circumstances for the validity of the magnetic dipole approximation of the perturbed field, induced by the presence of the object, are not fully understood. On the other hand, in the applied mathematics community, an asymptotic expansion of the perturbed magnetic field has been derived for small objects and a rigorous formula for the calculation of the MPT has been obtained. The purpose of this paper is to relate the results of the two communities, to provide a rigorous justification for the MPT, and to explain the situations in which the approximation is valid.**

***Index Terms*— Buried object detection, Eddy currents, magnetic induction, metal detectors, polarizability tensors.**

I. Introduction

THE characterization of a highly conducting object from the measurements of the low-frequency time harmonic magnetic field, which is perturbed by its presence, has important applications in metal detection, where the goal is to locate and identify a concealed conductive permeable inclusion in an otherwise low conducting background. Metal detectors are used in the search for artifacts of archaeological significance or of monetary value, the detection of landmines and unexploded ordnance, the recycling of metals, ensuring food safety, as well as in security screening at airports and public events. To improve their performance and reduce the number of false positives, there is considerable interest in the development of low-cost approaches and, in particular, the ability to characterize the shape, material properties, and frequency behavior of a conducting object by a small number of parameters using a symmetric rank 2 magnetic polarizability tensor (MPT) description. In the engineering community, the perturbed magnetic field response to the presence of a conducting permeable object and its interaction with a time harmonic background field is frequently approximated by a magnetic dipole. This, in turn, is approximated by the product of an MPT, which is independent of position, and the background field.

Wait [40] obtained an analytical solution that describes the response of a conducting permeable sphere to a uniform time harmonic background field. He found that the magnetic moment induced by the presence of the object takes a simple form consisting of a scalar, depending on the radius, conductivity, frequency, and permeability contrast of the object, multiplied by the uniform background field employed. Although no reference to an MPT is made, this does fit the aforementioned description. Here, the MPT is a scalar multiple of the identity tensor and the perturbed magnetic field resulting from the induced magnetic moment description, in this case, coincides with the exact representation of the perturbed field, as the alternative derivation in [38, p. 375] shows. An analytical solution for a conducting permeable sphere placed in a time harmonic background field generated by a coil, approximated as a dipole source, has also been obtained [41]. Here, the leading order term in the infinite series solution involves the same scalar function, which characterizes the sphere's radius, conductivity, and permeability for a given frequency, as found in the uniform excitation case. The case of a general sphere excited by a time harmonic dipole field has also been considered in [42]. Furthermore, Wait and Spies [43] have obtained an analytical expression for the perturbed magnetic field when a conducting permeable sphere is placed in a background field consisting of either a pulse or a step function. Their solution is in terms of a time-dependent operator, which can be expanded in terms of poles of a scalar transcendental equation.

The first mention of a rank 2 MPT appears to be in [20, p. 197] (note the Russian edition predates this English version). They state that the magnetic moment induced by a conductor can be expressed as a linear combination of the background magnetic field through a symmetric MPT. They further state that the MPT is complex valued, depends on the orientation of the object in the background field as well as its shape and the frequency of excitation. For simpler electro/magnetostatic problems, the representation of electric and magnetic moments in terms of background fields and electric/MPTs, which describe the shape and material contrast of dielectric and magnetic objects, is older still and related work on the depolarizing and demagnetization coefficients of ellipsoids has been published as early as in 1945 by Osborn [32] (see also [6], [19], [22], and [39]).

Baum has made considerable contributions to the description of conducting objects. He generalizes the work of Wait and Spies' on spheres to the description of the response from

Manuscript received November 20, 2017; revised January 8, 2018; accepted January 27, 2018. This work was supported by Engineering and Physical Science Research Council under Grant EP/R002134/1 and Grant EP/R002177/1. The work of W. R. B. Lionheart was supported by the Royal Society for a Challenge Grant and in part by a Wolfson Research Merit Award.
(Corresponding author: Paul D. Ledger.)

P. D. Ledger is with the College of Engineering, Swansea University Bay Campus, Swansea SA1 8EN, U.K. (e-mail: p.d.ledger@swansea.ac.uk).

W. R. B. Lionheart is with the School of Mathematics, The University of Manchester, Manchester M13 9PL, U.K.

Color versions of one or more of the figures in this paper are available online at http://ieeexplore.ieee.org.

Digital Object Identifier 10.1109/TGRS.2018.2801359

This work is licensed under a Creative Commons Attribution 3.0 License. For more information, see http://creativecommons.org/licenses/by/3.0/

a general conducting permeable object when the background field is transient. The complex analysis he performs results in a characterization of a conducting permeable object using a rank 2 MPT expressed as an infinite sum of poles associated with the object in consideration [9], [10]. He promotes this technique as the singularity expansion method and the poles of his MPTs as being a suitable means to characterize different conducting permeable objects [11] (for further details on the singularity expansion method, see [12] and references therein).

(Semi)analytical solutions have been derived for the magnetoquasi-static response for a conducting permeable spheroid placed in a uniform time harmonic background magnetic field under axial excitation [14] by the group of O'Neill. In the case of excitation at a frequency close to the quasi-static limit, the group employs a type of impedance boundary condition in order to simplify the treatment of the transmission conditions and avoid the challenging problem of small skin depths and interior–exterior coupling of the field equations. The perturbed magnetic field due to the presence of a conducting permeable spheroid is obtained from the leading order term in a multipole expansion, and by considering the induced magnetic moment for this object, the diagonal component of the MPT associated with the axial excitation can be identified. The group has generalized this to the treatment of spheroids excited by background fields of arbitrary orientation, thereby allowing the identification of the other diagonal MPT coefficients [7], and has explored how the MPT coefficients vary over a broadband frequency range in [8]. This has been extended still further to the treatment of conducting permeable ellipsoids in [17]. These (semi)analytical solutions involve truncated infinite series solution involving Legendre and Bessel functions, and to overcome this complexity, a simpler treatment involving perfectly conducting spheroids has been presented in [31], where the excitation is by a time harmonic background magnetic field generated by a coil rather than a uniform field.

The group of Shubitidze has developed the method of auxiliary sources [34], [36], [37] as a low-cost approach to describe the field perturbations caused by the presence of general conducting permeable objects. They introduce point and surface charges on imaginary surfaces, which are usually chosen to be conformal to the object's surface and located on both its interior and exterior, and develop an approximate integral equation solution. When applied to eddy-current problems [36], [37], the group assumes the perturbed magnetic field to be irrotational in the nonconducting background medium, so that it can be expressed as the gradient of a scalar potential. However, this is only true for simply connected objects, and for multiply connected objects with loops (e.g., a torus or ring), the unbounded region surrounding the object is also multiply connected and there are curl free magnetic fields in this region that cannot be expressed as the gradient of a scalar potential. These loop fields remain present at large distances from the object and consequently their approach is not applicable to such objects (see [13], [22, Proof of Lemma 1], and references therein, which give a full explanation in terms of Betti numbers). In addition, the reduction in the governing curl–curl equation in the interior of the object to a vector Helmholtz equation, by the assumption of a solenoidal magnetic field, is only correct if the object has a smooth boundary and is not valid for general objects that may have sharp edges and corners. More recently, the group of Shubitidze has subsequently extended the method of auxiliary sources to apply it to heterogeneous objects and objects placed in a background media that are conductive (e.g., sea water) [34]. Their more recent work does not require the eddy approximation to made, so that it can be applied to objects excited by higher frequency background fields.

For practical object classification using an MPT, its coefficients need to be related to field measurements. Multiple measurements are required in order to reliably *fit* the tensor to the data and alternative approaches can be conceived. One possibility is to have a single exciter and a single measurement coil and to take measurements at a large number of different positions (and orientations) by either fixing the exciter and moving the measurement coil or moving them together in a fixed unit (such as in a hand-held metal detector) [15]. Here, ideas (and terminology) can be borrowed from the radar cross section (RCS) in electromagnetic scattering where bistatic involves a fixed exciter and moving the receiver and monostatic involves keeping a fixed exciter–receiver distance. Another approach is to have an array of coils, where one coil is excited at a time and the others are used for taking the measurements [24], [35], which, in the context of RCS, would be multistatic. Indeed, there is a further connection between the MPT in metal detection and the RCS pattern of an object. The latter describes the far-field power of waves scattered by an object and can be approximated in terms of a different class of polarizability tensors, which provide an approach to object characterization at higher frequencies (see [22] and references therein for further details).

Techniques involving MPTs (and those closely related to it) have been applied to a variety of applications. Electromagnetic induction spectroscopy [30] is a related empirical technique, where the focus is on the broadband frequency response to a given waveform, rather than a simple time harmonic signal, and has been applied to landmine clearance. The simultaneous identification of multiple unexploded ordnance has been considered in [18], where an MPT representation, in which the coupling between the eddy currents in multiple bodies is neglected, has been applied. The group of Peyton has applied real-time MPT inversion and classification of multiple objects to the problem of security screening [26]–[29], [45] and is developing techniques for measuring MPTs for a range of threat and nonthreat items illuminated by harmonic fields, in the lab [1], [16] and field. The group of Bilas and Vasić has also made field measurements of MPTs for a range of objects using harmonic and impulse excitation [2] and is developing systems for mine clearance in partnership with the group of Peyton.

Despite the considerable attention, the MPT has received in the engineering literature an explicit formula for its calculation for arbitrary-shaped object is, to the best of our knowledge, not available. (Semi)analytical solutions are only available for spheres and ellipsoids with the latter requiring approximations to be made. Engineers are aware that the dipole approximation works well for excitation by uniform fields and coincides with the exact description for a spherical object, but its accuracy for other objects is unclear. The magnetic dipole approximation has also been shown to work well when the excitation is by a current carrying coil placed sufficiently far from the object, but a rigorous justification of the constraints required (on the material parameters, object size, and frequency), in order for it to apply, does not appear to be available. In contrast, in the applied mathematics community, an asymptotic formula for the perturbed magnetic field for the eddy-current problem of a conducting (permeable) object in a low-frequency time harmonic background field has been rigorously derived for the case where the object size tends to zero [4], [5]. For this case, an explicit formula for the computation of the MPT coefficients has also been derived [21], [22] and our previous analysis clearly states what the requirements are on the material parameters, frequency, and object size in order for it to apply. In these articles, we have described how the MPT coefficients can be computed for a general-shaped object and included a range of illustrative examples to show that our computations agree with both known analytical solutions and experimental data. We have shown how the MPT transforms under the rotation of an object and also how the number of independent complex coefficients of an MPT can be much fewer than six if the object has rotational and/or mirror symmetries.

The purpose of this paper is to relate the results of the electrical engineering and applied mathematics communities, to provide a rigorous justification for the MPT, and to explain the situations in which the approximation is valid. We begin, in Section II, with the key equations that describe the underlying eddy-current model, which describe the field perturbation caused by the presence of a conducting permeable object. Then, in Section III, we discuss different alternative approaches for representing the perturbed magnetic field in the presence of such an object. In Section IV, we establish the validity of engineering approach for the MPT and explain when the approximation is valid. Then, in Section V, we apply the asymptotic formula to a series of realistic metal detection scenarios. We close with some concluding remarks, which justify the validity of the multipole expansion and its connection with the aforementioned asymptotic expansion.

II. Eddy-Current Model

We set the scene by recalling the eddy-current model that describes the electromagnetic fields in the metal detection problem. In the presence of a highly conducting object B_α (i.e., the target) with homogenous conductivity σ_* and permeability μ_*, the magnetic and electric interaction fields, $\boldsymbol{H}_\alpha$ and $\boldsymbol{E}_\alpha$, respectively, satisfy the eddy-current equations

$$\nabla \times \boldsymbol{E}_\alpha = \mathrm{i}\omega\mu_* \boldsymbol{H}_\alpha, \quad \nabla \times \boldsymbol{H}_\alpha = \sigma_* \boldsymbol{E}_\alpha \tag{1}$$

in B_α where $\mathrm{i} := \sqrt{-1}$ and $\omega := 2\pi f$ is the angular frequency. For the aforementioned applications, the background medium is either nonconducting or its conductivity is significantly less than that of B_α and, therefore, the region $B_\alpha^c := \mathbb{R}^3 \setminus B_\alpha$ surrounding the object is assumed to be an unbounded region of nonconducting region free space. In this region, the fields satisfy

$$\nabla \times \boldsymbol{E}_\alpha = \mathrm{i}\omega\mu_0 \boldsymbol{H}_\alpha, \quad \nabla \times \boldsymbol{H}_\alpha = \boldsymbol{J}_0 \tag{2}$$

where $\boldsymbol{J}_0$ is an external current source and μ_0 is the permeability of free space. The two regions are coupled by the transmission conditions

$$[\boldsymbol{n} \times \boldsymbol{E}_\alpha]_{\Gamma_\alpha} = [\boldsymbol{n} \times \boldsymbol{H}_\alpha]_{\Gamma_\alpha} = \boldsymbol{0} \tag{3}$$

where $[\cdot]_{\Gamma_\alpha}$ denotes the jump, which applies on the surface of the object $\Gamma_\alpha := \partial B_\alpha$. In addition, the fields satisfy suitable decay conditions as $|\boldsymbol{x}| \to \infty$[1] and the model is completed by the requirement that $\nabla \cdot \boldsymbol{E}_\alpha = 0$ in B_α^c. Combining (1)–(3) and the aforementioned conditions represents a transmission problem that needs to be solved for $\boldsymbol{E}_\alpha$ and $\boldsymbol{H}_\alpha$. In the absence of the object, the transmission problem simplifies to finding the background fields $\boldsymbol{E}_0$ and $\boldsymbol{H}_0$ that satisfy (2) with $\alpha = 0$ in $\mathbb{R}^3$ and decay as $|\boldsymbol{x}| \to \infty$. If the excitation is instead by a background field $\boldsymbol{H}_0$, which is known and uniform in $\mathbb{R}^3$, and $\boldsymbol{E}_0$ is a corresponding known linear field, the transmission problem for $\boldsymbol{E}_\alpha$ and $\boldsymbol{H}_\alpha$ takes a similar form except that $\boldsymbol{J}_0 = \boldsymbol{0}$ and the decay conditions become $(\boldsymbol{E}_\alpha - \boldsymbol{E}_0)(\boldsymbol{x}) = O\ (1/|\boldsymbol{x}|)$ and $(\boldsymbol{E}_\alpha - \boldsymbol{H}_0)(\boldsymbol{x}) = O(1/|\boldsymbol{x}|)$ as $|\boldsymbol{x}| \to \infty$.

To assist with the detection and location of a conducting object from field measurements, the task is to find an expression for the perturbed magnetic field $(\boldsymbol{H}_\alpha - \boldsymbol{H}_0)(\boldsymbol{x})$, with $\boldsymbol{x}$ exterior to the object, which characterizes B_α in terms of a small number of parameters independent of its position. In the following, we consider excitation both by a current source and by a uniform background field.

III. Representation and Approximation of the Perturbed Field

To be able to characterize the shape and material properties of an object, independent of its position, an approximate method for representing $(\boldsymbol{H}_\alpha - \boldsymbol{H}_0)(\boldsymbol{x})$ for $\boldsymbol{x}$ outside the object is needed. We begin with the multipole representation of the perturbed magnetic field, $(\boldsymbol{H}_\alpha - \boldsymbol{H}_0)(\boldsymbol{x})$, which is well known in the engineering community. We also present an exact representation of the perturbed field and an asymptotic expansion valid for a small object.

A. Multipole Expansion

In the engineering community, $(\boldsymbol{H}_\alpha - \boldsymbol{H}_0)(\boldsymbol{x})$, for $\boldsymbol{x}$ exterior to the object, is frequently approximated by a multipole expansion and, in particular, by the term associated with an equivalent magnetic dipole, which, in orthonormal coordinates, has the form

$$\begin{aligned}(\boldsymbol{H}_\alpha - \boldsymbol{H}_0)(\boldsymbol{x})_i &\approx \frac{1}{4\pi r^3}(3\hat{\boldsymbol{r}} \otimes \hat{\boldsymbol{r}} - \mathbb{I})_{ij}(\boldsymbol{m})_j \\ &= \left(\boldsymbol{D}_x^2 G(\boldsymbol{x}, \boldsymbol{z})\right)_{ij} \boldsymbol{m}_j \end{aligned}\tag{4}$$

[1] $\boldsymbol{E} = O(1/|\boldsymbol{x}|)$ and $\boldsymbol{H} = O(1/|\boldsymbol{x}|)$ as $|\boldsymbol{x}| \to \infty$, here the big O-Landau notation implies that the fields go to 0 at least as fast as $1/|\boldsymbol{x}|$ but can be quicker in practice.

This article has been accepted for inclusion in a future issue of this journal. Content is final as presented, with the exception of pagination.

where $\boldsymbol{m}$ is a constant magnetic dipole moment, which is chosen assuming that the response resembles a magnetic dipole. Furthermore, as shown in Fig. 1(a), $\boldsymbol{x} = \boldsymbol{r}+\boldsymbol{z}$, with $\boldsymbol{r}$ denoting a coordinate measured from the center of the object, $\boldsymbol{z}$ denoting the position of the center of the object relative to the origin, and $\hat{\boldsymbol{r}} = \boldsymbol{r}/r$, $r = |\boldsymbol{r}|$. Einstein summation convention has also been used[2] and has included an alternative form involving the free space Laplace Green's function $G(\boldsymbol{x},\boldsymbol{z}) := 1/(4\pi|\boldsymbol{x}-\boldsymbol{z}|)$ for later comparison.

Rewriting (1) in the alternative form

$$\nabla \times \boldsymbol{E}_\alpha = \mathrm{i}\omega\mu_0(\boldsymbol{H}_\alpha + \boldsymbol{M}_\alpha), \quad \nabla \times \boldsymbol{H}_\alpha = \boldsymbol{J}_\alpha^e \tag{5}$$

it is clear that the magnetization $\boldsymbol{M}_\alpha := ((\mu_*/\mu_0) - 1)\boldsymbol{H}_\alpha$ is nonzero for a permeable object and the eddy current $\boldsymbol{J}_\alpha^e := \sigma_*\boldsymbol{E}_\alpha$ is nonzero for a conducting object. Replacing the presence of B_α by an equivalent magnetization and induced eddy current, as shown in Fig. 1(b), the induced magnetic dipole moment, such that (4) provides a reasonable approximation, takes the form

$$\boldsymbol{m} := \frac{1}{2}\int_{B_\alpha} \boldsymbol{r}' \times \boldsymbol{J}_\alpha^e(\boldsymbol{r}')d\boldsymbol{r}' + \int_{B_\alpha} \boldsymbol{M}_\alpha(\boldsymbol{r}')d\boldsymbol{r}', \tag{6}$$

$$= \frac{\sigma_*}{2}\int_{B_\alpha} \boldsymbol{r}' \times \boldsymbol{E}_\alpha(\boldsymbol{r}')d\boldsymbol{r}' + \left(\frac{\mu_*}{\mu_0} - 1\right)\int_{B_\alpha} \boldsymbol{H}_\alpha(\boldsymbol{r}')d\boldsymbol{r}'. \tag{7}$$

In the context of magnetostatics, Jackson [19, p. 180] states that such a construction for $\boldsymbol{m}$ is expected to give an accurate representation for small distributions of current,[3] which hints that the object size needs to be small, but no further information about how the approximation in (4) depends on the object's size is available.

As outlined in the introduction, it is often assumed (without proof) that

$$(\boldsymbol{m})_j = (\mathcal{M})_{jk}(\boldsymbol{H}_0|_{B_\alpha})_k \tag{8}$$

where $\mathcal{M}$ is the rank 2 MPT and the background magnetic field $\boldsymbol{H}_0|_{B_\alpha}$ is some assumed evaluation of the background field. The MPT has been postulated to depend on the shape and size of B_α and ω, σ_*, and μ_*/μ_0, but to be independent of the object's position. In the case of excitation by a uniform field, Landau and Lifshitz [20] motivate (8) by realizing that $\boldsymbol{m}$ will be a linear function of the constant complex amplitude $\boldsymbol{H}_0$. But, for nonuniform $\boldsymbol{H}_0$, it is not clear whether (8) still applies or how $\boldsymbol{H}_0|_{B_\alpha}$ should be evaluated.

In the case of a conducting permeable sphere of radius α excited by a uniform field, an explicit analytical solution is available. For this case, it can be shown that (4) and (8) become exact, and $\mathcal{M}$ is diagonal and has coefficients

[2]We use the notation $\boldsymbol{e}_i$ to denote the ith orthonormal unit vector. Repeated indices imply summation so that the ith coefficient of a vector $\boldsymbol{a}$ is $(\boldsymbol{a})_i$ and $\boldsymbol{a} = (\boldsymbol{a})_i\boldsymbol{e}_i$; furthermore, a rank 2 tensor, for which we use a calligraphic font, can be written as $\mathcal{M} = (\mathcal{M})_{ij}\boldsymbol{e}_i \otimes \boldsymbol{e}_j$, where $(\mathcal{M})_{ij}$ denotes its coefficients.

[3]With small being relative to the scale of length of interest to the observer.

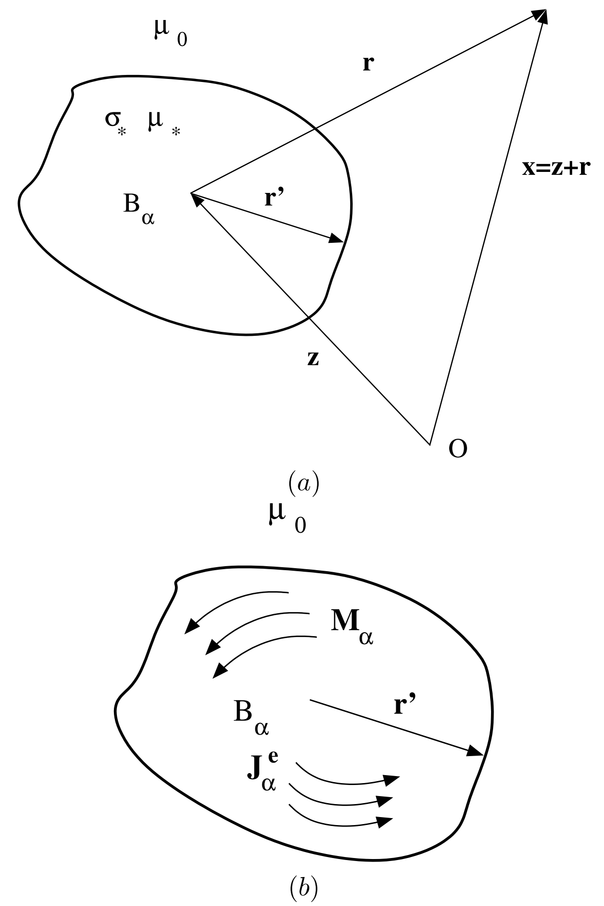

Fig. 1. Illustration of the conducting object B_α showing (a) configuration of the coordinate system and (b) representation in terms of an equivalent (eddy) current $\boldsymbol{J}_\alpha^e$ and magnetization $\boldsymbol{M}_\alpha$.

$(\mathcal{M})_{\ell i} = M\delta_{\ell i}$ where [38], [40][4]

$$\overline{M} = 2\pi\alpha^3 \frac{((2\mu_* + \mu_0)\upsilon I_{-1/2} - (\mu_0(1+\upsilon^2) + 2\mu_*)I_{1/2})}{(\mu_* - \mu_0)\upsilon I_{-1/2} + (\mu_0(1+\upsilon^2) - \mu_*)I_{1/2}} \tag{9}$$

where $\upsilon := \alpha(\mathrm{i}\sigma_*\mu_*\omega)^{1/2}$, $I_{1/2}(\upsilon) = (2/\pi\upsilon)^{1/2}\sinh\upsilon$, and $I_{-1/2}(\upsilon) = (2/\pi\upsilon)^{1/2}\cosh\upsilon$. Note that the overline indicates the complex conjugate, which appears due to the $e^{\mathrm{i}\omega t}$ time variation in [38] rather than the $e^{-\mathrm{i}\omega t}$ assumed here. When a conducting sphere is placed in a background field generated by a coil, the exact result for $(\boldsymbol{H}_\alpha - \boldsymbol{H}_0)(\boldsymbol{x})$ is instead an infinite series solution [42]. However, when the radius of the coil is small compared with the distance from the sphere, the leading order dipole term dominates and the sphere's characteristics are again described by the same scalar as given in (9). Approximate analytical solutions have also been found for spheroids [7], [8], [14] and ellipsoids [17] when placed in a uniform field, which have been obtained by using an impedance boundary condition.

For general objects, the coefficients of $\mathcal{M}$ are usually found through fitting them to physical (or computational) measurements of the perturbed field for an object placed in

[4]The definition of a_0 in [40, eq. (7)] is equivalent to $M|\boldsymbol{H}_0|/\pi$ in this paper.

This article has been accepted for inclusion in a future issue of this journal. Content is final as presented, with the exception of pagination.

a series of uniform fields that are orientated in the directions $\boldsymbol{e}_i$, $i = 1, 2, 3$, in turn [15], [28], [30], [33].

B. Exact Representation

Although (4) is commonly quoted in the engineering literature, it must be remembered that, apart from in exceptional situations, this does not represent the exact $(\boldsymbol{H}_\alpha - \boldsymbol{H}_0)(\boldsymbol{x})$. The exact field perturbation for $\boldsymbol{x}$ exterior to the object is via the representation formula [4]

$$(\boldsymbol{H}_\alpha - \boldsymbol{H}_0)(\boldsymbol{x}) = \int_{B_\alpha} \nabla_x G(\boldsymbol{x}, \boldsymbol{y}) \times \nabla_y \times (\boldsymbol{H}_\alpha - \boldsymbol{H}_0) d\boldsymbol{y} + \left(\frac{\mu_*}{\mu_0} - 1\right) \int_{B_\alpha} \boldsymbol{D}_x^2 G(\boldsymbol{x}, \boldsymbol{y}) \boldsymbol{H}_\alpha d\boldsymbol{y} \quad (10)$$

where $\boldsymbol{y}$ is measured from the origin (note this need not be inside the object) and used to perform integration over B_α. We emphasize that (10) is a coupled equation with the magnetic interaction field $\boldsymbol{H}_\alpha$ appearing on both sides and requires the solution of the transmission problem described in Section II for its exact evaluation. In the case of small objects, care must be taken when deciding how to approximate the integrals as both the first and second derivatives of the Green's function and the fields are functions of position inside the object. For instance, consider the case of a nonconducting object so that the problem simplifies to that of determining $(\boldsymbol{H}_\alpha - \boldsymbol{H}_0)(\boldsymbol{x})$ for a permeable object in magnetostatics. Here, a similarity between (10) and combining (4) and (7) can be seen, where $\boldsymbol{D}_x^2\ G(\boldsymbol{x}, \boldsymbol{y})$, which appears under the integral sign in (10), has been approximated by its value at the object's center [i.e., $\boldsymbol{D}_x^2\ G(\boldsymbol{x}, \boldsymbol{z})$ in (4)], but (4) does not provide any measure of accuracy of this approximation.

C. Asymptotic Expansion

In the applied mathematics community, the object is described as $B_\alpha = \alpha B + \boldsymbol{z}$, which means that it can be thought of a unit-sized object B located at the origin, scaled by α and translated by $\boldsymbol{z}$. The asymptotic formula for $\boldsymbol{x}$ away from B_α

$$(\boldsymbol{H}_\alpha - \boldsymbol{H}_0)(\boldsymbol{x})_i = \left(\boldsymbol{D}_x^2\ G(\boldsymbol{x}, \boldsymbol{z})\right)_{ij} (\mathcal{M})_{jk} (\boldsymbol{H}_0(\boldsymbol{z}))_k + (\boldsymbol{R}(\boldsymbol{x}))_i \quad (11)$$

which holds as the object's size $\alpha \to 0$ has been rigorously derived from (10) for the case of $\nu := \alpha^2 \sigma_* \mu_0 \omega = O(1)$ in [4] and [21]. This is not as restrictive as it may appear since $\nu = O(1)$ implies that $\nu \leq C$ for some finite constant C, i.e., we require that ν remains bounded as $\alpha \to 0$. The case of fixed σ_* and ω as $\alpha \to 0$ also satisfies this requirement. This technical restriction is necessary so that the eddy-current model is not invalidated when choosing σ_* and ω for a given α. Importantly, (11) provides not only a leading order term that is computable but also a measure of accuracy of the approximation, since [4] and [21] show that $\boldsymbol{R}(\boldsymbol{x}) = O(\alpha^4)$.

To better understand (11), consider how, in the engineering literature, an eddy current problem is often interpreted in terms of primary and secondary magnetic fields. The primary field is the background magnetic field $\boldsymbol{H}_0$ and is often viewed as being responsible for the generation of eddy currents inside the object. The secondary magnetic field is viewed as that which is generated by the presence of eddy currents inside object. In reality, such secondary magnetic fields can induce further eddy currents inside the object, but engineers usually assume this effect can be neglected. The quantity $(\boldsymbol{H}_\alpha - \boldsymbol{H}_0)(\boldsymbol{x})$ describes all the field perturbations due to the presence of the object and formula (11) expresses the fact that these are due to a contribution of what engineers call the secondary magnetic field (the first term on the right-hand side) plus other effects. The residual $\boldsymbol{R}(\boldsymbol{x})$ measures how well the secondary fields approximate the true $(\boldsymbol{H}_\alpha - \boldsymbol{H}_0)(\boldsymbol{x})$.

The complex symmetric rank 2 tensor $\mathcal{M}$, which appears in (11), is the MPT and we have previously shown that it can be constructed as $\mathcal{M} := -\mathcal{C} + \mathcal{N}$[5] for a general-shaped object [21], [22]. The coefficients of $\mathcal{C}$ and $\mathcal{N}$ depend on ω, σ_*, μ_*/μ_0, α, and the shape of B and we will present the explicit formula for $\mathcal{C}$ and $\mathcal{N}$ again in (23) later in this paper. In [22], we have presented numerical results for the frequency behavior of the coefficients of $\mathcal{M}$ for a range of simply and multiply connected objects. Our previously presented results have exhibited excellent agreement with MPTs previously presented in the electrical engineering literature. Our results also show how the coefficients of $\mathcal{M}$ tend to $\mathcal{T}(\mu_r)$ when $\omega \to 0$ and to $\mathcal{T}(0)$ when $\sigma_* \to \infty$ and the object is simply connected. Here, $\mathcal{T}$ is the Pólya–Szegö tensor and when parameterized by μ_r and 0, it describes the response from a magnetostatic and perfectly conducting object, respectively.

A generalization of (11) has recently been derived [23], which extends the leading order term to a complete asymptotic expansion of the perturbed field. The higher order terms are expressed in terms of a new class of (higher rank) generalized MPTs (GMPTs) and higher order derivatives of $G(\boldsymbol{x}, \boldsymbol{z})$ and $\boldsymbol{H}_0(\boldsymbol{z})$. This expansion allows the perturbed field to be represented more accurately and the GMPTs allow the object's shape and material characteristics and frequency behavior to be better characterized.

IV. Derivation of an Explicit Formula for $\mathcal{M}$

In this section, we present a derivation for an explicit formula for the coefficients of $\mathcal{M}$, which, we will show, agrees with our previous result. The presented derivation is intended to be more accessible to the engineering community and will also asses the validity of (4) and (8).

A. Validity of (4)

The accuracy of the approximation in (4) will depend on the size of the object and on the parameter ν previously introduced. To make this clear, we write $B_\alpha = \alpha B + \boldsymbol{z}$ and rewrite (10) in the form of

$$\begin{aligned}(\boldsymbol{H}_\alpha - \boldsymbol{H}_0)(\boldsymbol{x})_i &= \mathrm{i}\alpha^3 \sigma_* \omega \int_B (\nabla_x G(\boldsymbol{x}, \alpha\boldsymbol{\xi} + \boldsymbol{z}) \times \boldsymbol{A}_\alpha(\alpha\boldsymbol{\xi} + \boldsymbol{z}))_i d\boldsymbol{\xi} \\ &\quad + \alpha^3 \left(\frac{\mu_*}{\mu_0} - 1\right) \int_B \boldsymbol{D}_x^2 G(\boldsymbol{x}, \alpha\boldsymbol{\xi} + \boldsymbol{z})_{ij} \\ &\quad \mu_*^{-1} (\nabla \times \boldsymbol{A}_\alpha(\alpha\boldsymbol{\xi} + \boldsymbol{z}))_j d\boldsymbol{\xi} \quad (12)\end{aligned}$$

[5]In this paper, we have dropped a double check on $\mathcal{M}$ and a single check on $\mathcal{C}$ compared with the notation in [21] and [22] so as to simplify the notation.

This article has been accepted for inclusion in a future issue of this journal. Content is final as presented, with the exception of pagination.

which is still exact and where we have introduced a vector potential such that $\boldsymbol{E}_\alpha(\boldsymbol{x}) = \mathrm{i}\omega \boldsymbol{A}_\alpha(\boldsymbol{x})$ in B_α and $\mu \boldsymbol{H}_\alpha = \nabla \times \boldsymbol{A}_\alpha$ in $\mathbb{R}^3$. The vector potential $\boldsymbol{A}_\alpha$ satisfies the transmission problem

$$\begin{aligned}
\nabla \times \mu_*^{-1} \nabla \times \boldsymbol{A}_\alpha &= \mathrm{i}\omega\sigma_* \boldsymbol{A}_\alpha && \text{in } B_\alpha && \text{(13a)}\\
\nabla \cdot \boldsymbol{A}_\alpha &= 0 && \text{in } B_\alpha^c && \text{(13b)}\\
\nabla \times \mu_0^{-1} \nabla \times \boldsymbol{A}_\alpha &= \boldsymbol{0} && \text{in } B_\alpha^c && \text{(13c)}\\
[\boldsymbol{n} \times \boldsymbol{A}_\alpha]_{\Gamma_\alpha} &= \boldsymbol{0} && \text{on } \Gamma_\alpha := \partial B_\alpha && \text{(13d)}\\
[\boldsymbol{n} \times \mu^{-1} \nabla \times \boldsymbol{A}_\alpha]_{\Gamma_\alpha} &= \boldsymbol{0} && \text{on } \Gamma_\alpha && \text{(13e)}\\
\mu_0^{-1} \nabla_x \times \boldsymbol{A}_\alpha - \boldsymbol{H}_0 &= O(|\boldsymbol{x}|^{-1}) && \text{as } |\boldsymbol{x}| \to \infty && \text{(13f)}
\end{aligned}$$

in the case of excitation by a uniform background field and

$$\begin{aligned}
\nabla \times \mu_*^{-1} \nabla \times \boldsymbol{A}_\alpha &= \mathrm{i}\omega\sigma_* \boldsymbol{A}_\alpha && \text{in } B_\alpha && \text{(14a)}\\
\nabla \cdot \boldsymbol{A}_\alpha &= 0 && \text{in } B_\alpha^c && \text{(14b)}\\
\nabla \times \mu_0^{-1} \nabla \times \boldsymbol{A}_\alpha &= \boldsymbol{J}_0 && \text{in } B_\alpha^c && \text{(14c)}\\
[\boldsymbol{n} \times \boldsymbol{A}_\alpha]_{\Gamma_\alpha} &= \boldsymbol{0} && \text{on } \Gamma_\alpha && \text{(14d)}\\
[\boldsymbol{n} \times \mu^{-1} \nabla \times \boldsymbol{A}_\alpha]_{\Gamma_\alpha} &= \boldsymbol{0} && \text{on } \Gamma_\alpha && \text{(14e)}\\
\boldsymbol{A}_\alpha &= O(|\boldsymbol{x}|^{-1}) && \text{as } |\boldsymbol{x}| \to \infty && \text{(14f)}
\end{aligned}$$

in the case of excitation by background field produced by a current source. Both of these problems can be easily derived from the governing equations in Section II. Next, we introduce the following Taylor's series approximations for $\boldsymbol{x}$ external to B_α, $\boldsymbol{y} = \alpha\boldsymbol{\xi} + \boldsymbol{z}$ in B_α, and $\boldsymbol{\xi}$ in B:

$$\begin{aligned}
\boldsymbol{D}_x^2 G(\boldsymbol{x}, \boldsymbol{y}) &= \boldsymbol{D}_x^2 G(\boldsymbol{x}, \boldsymbol{z}) + O(\alpha) && \text{(15a)}\\
\nabla_x G(\boldsymbol{x}, \boldsymbol{y}) &= \nabla_x G(\boldsymbol{x}, \boldsymbol{z}) - \boldsymbol{D}_x^2 G(\boldsymbol{x}, \boldsymbol{z})(\alpha\boldsymbol{\xi}) + O(\alpha^2) && \text{(15b)}
\end{aligned}$$

as $\alpha \to 0$. These expansions are then substituted into (12) and Appendix A shows for $\boldsymbol{x}$ away from B_α that

$$\begin{aligned}
(\boldsymbol{H}_\alpha - \boldsymbol{H}_0)(\boldsymbol{x})_i
&= \frac{\mathrm{i}\alpha^4 \sigma_* \omega}{2} \left(\boldsymbol{D}_x^2 G(\boldsymbol{x}, \boldsymbol{z})\right)_{ij} \int_B (\boldsymbol{\xi} \times (\boldsymbol{A}_\alpha(\alpha\boldsymbol{\xi} + \boldsymbol{z})))_j \, d\boldsymbol{\xi}\\
&\quad + \alpha^3 \left(\frac{\mu_*}{\mu_0} - 1\right) \left(\boldsymbol{D}_x^2 G(\boldsymbol{x}, \boldsymbol{z})\right)_{ij}\\
&\quad \int_B \mu_*^{-1} (\nabla \times \boldsymbol{A}_\alpha(\alpha\boldsymbol{\xi} + \boldsymbol{z}))_j \, d\boldsymbol{\xi} + (\boldsymbol{R}_d(\boldsymbol{x}))_i \qquad (16)
\end{aligned}$$

where Einstein summation convention has been applied. Noting that $\boldsymbol{r}' = \alpha\boldsymbol{\xi}$ it easily follows from (16), for the particular case, where $B_\alpha = \alpha B + \boldsymbol{z}$ and $\boldsymbol{m}$ is given by (7) that:

$$\begin{aligned}
(\boldsymbol{H}_\alpha - \boldsymbol{H}_0)(\boldsymbol{x})_i &= \left(\boldsymbol{D}_x^2 G(\boldsymbol{x}, \boldsymbol{z})\right)_{ij}\\
&\quad \left(\frac{\sigma_*}{2} \int_{B_\alpha} (\boldsymbol{r}' \times \boldsymbol{E}_\alpha(\boldsymbol{r}'))_j \, d\boldsymbol{r}' \right.\\
&\quad \left. + \left(\frac{\mu_*}{\mu_0} - 1\right) \int_{B_\alpha} (\boldsymbol{H}_\alpha(\boldsymbol{r}'))_j \, d\boldsymbol{r}' \right) + (\boldsymbol{R}_d(\boldsymbol{x}))_i\\
&= \left(\boldsymbol{D}_x^2 G(\boldsymbol{x}, \boldsymbol{z})\right)_{ij} (\boldsymbol{m})_j + (\boldsymbol{R}_d(\boldsymbol{x}))_i. \qquad (17)
\end{aligned}$$

We immediately see that the first term in (17) has the same form as in (4), but, for this to be a meaningful approximation, the residual $\boldsymbol{R}_d(\boldsymbol{x})$ needs to be small in comparison and $\boldsymbol{x}$ needs to be away from B_α.

Before we can address the situations in which $\boldsymbol{R}_d(\boldsymbol{x})$ is small, we notice, from (16), that the first two terms involve different powers of α implying there must be some relationship between σ_*, α, and ω, which is hidden when the alternative form (17) is used. Since the object size needs to be small for (15) to hold, we demand that the first two terms in (16) involve the same power of α. To achieve this, we first introduce the reduced vector potential $\boldsymbol{A}_r(\boldsymbol{x}) := (\boldsymbol{A}_\alpha - \boldsymbol{A}_0)(\boldsymbol{x})$, with $\boldsymbol{A}_0$ being the corresponding vector potential in the absence of the object, which satisfies the transmission problem

$$\begin{aligned}
\nabla \times \mu_*^{-1} \nabla \times \boldsymbol{A}_r &= \mathrm{i}\omega\sigma_* (\boldsymbol{A}_0 + \boldsymbol{A}_r) && \text{in } B_\alpha && \text{(18a)}\\
\nabla \cdot \boldsymbol{A}_r &= 0 && \text{in } B_\alpha^c && \text{(18b)}\\
\nabla \times \mu_0^{-1} \nabla \times \boldsymbol{A}_r &= \boldsymbol{0} && \text{in } B_\alpha^c && \text{(18c)}\\
[\boldsymbol{n} \times \boldsymbol{A}_r]_{\Gamma_\alpha} &= \boldsymbol{0} && \text{on } \Gamma_\alpha && \text{(18d)}\\
[\boldsymbol{n} \times \mu^{-1} \nabla \times \boldsymbol{A}_r]_{\Gamma_\alpha} &= -[\mu^{-1}]_{\Gamma_\alpha} \boldsymbol{n} \times \nabla \times \boldsymbol{A}_0 && \text{on } \Gamma_\alpha && \text{(18e)}\\
\boldsymbol{A}_r &= O(|\boldsymbol{x}|^{-1}) && \text{as } |\boldsymbol{x}| \to \infty. && \text{(18f)}
\end{aligned}$$

Note that the introduction of $\boldsymbol{A}_r$ allows the background field $\boldsymbol{H}_0$ in (13) and the current source $\boldsymbol{J}_0$ in (14) to be eliminated and instead $\boldsymbol{A}_0$ appears as a source term in B_α in both the cases. Second, we use a coordinate transformation followed by a scaling and set $\boldsymbol{A}_\Delta(\boldsymbol{\xi}) := \alpha \boldsymbol{A}_r((\boldsymbol{x} - \boldsymbol{z})/\alpha)$, which satisfies:

$$\begin{aligned}
\nabla_\xi \times \mu_*^{-1} \nabla_\xi \times \boldsymbol{A}_\Delta &= \mathrm{i}\omega\sigma_*\alpha^2 \boldsymbol{A}_\Delta + \mathrm{i}\omega\sigma_*\alpha^2\alpha^{-1} &&\\
&\quad \boldsymbol{A}_0(\alpha\boldsymbol{\xi} + \boldsymbol{z}) && \text{in } B && \text{(19a)}\\
\nabla_\xi \cdot \boldsymbol{A}_\Delta &= 0 && \text{in } B^c && \text{(19b)}\\
\nabla_\xi \times \mu_0^{-1} \nabla_\xi \times \boldsymbol{A}_\Delta &= \boldsymbol{0} && \text{in } B^c && \text{(19c)}\\
[\boldsymbol{n} \times \boldsymbol{A}_\Delta]_\Gamma &= \boldsymbol{0} && \text{on } \Gamma && \text{(19d)}\\
[\boldsymbol{n} \times \mu^{-1} \nabla_\xi \times \boldsymbol{A}_\Delta]_\Gamma &= -[\mu^{-1}]_\Gamma \boldsymbol{n} \times \nabla &&\\
&\quad \times \boldsymbol{A}_0(\alpha\boldsymbol{\xi} + \boldsymbol{z}) && \text{on } \Gamma && \text{(19e)}\\
\boldsymbol{A}_\Delta &= O(|\boldsymbol{\xi}|^{-1}) && \text{as } |\boldsymbol{\xi}| \to \infty && \text{(19f)}
\end{aligned}$$

where $\Gamma := \partial B$ and $B^c := \mathbb{R}^3 \setminus B$. Writing (16) in terms of $\boldsymbol{A}_\Delta$ and $\boldsymbol{A}_0$ leads to the result

$$\begin{aligned}
(\boldsymbol{H}_\alpha - \boldsymbol{H}_0)(\boldsymbol{x})_i
&= \frac{\mathrm{i}\alpha^3 \nu}{2\mu_0} \left(\boldsymbol{D}_x^2 G(\boldsymbol{x}, \boldsymbol{z})\right)_{ij}\\
&\quad \int_B (\boldsymbol{\xi} \times (\boldsymbol{A}_\Delta(\boldsymbol{\xi}) + \alpha^{-1} \boldsymbol{A}_0(\alpha\boldsymbol{\xi} + \boldsymbol{z})))_j \, d\boldsymbol{\xi}\\
&\quad + \alpha^3 \left(\frac{\mu_*}{\mu_0} - 1\right) \left(\boldsymbol{D}_x^2 G(\boldsymbol{x}, \boldsymbol{z})\right)_{ij}\\
&\quad \int_B \mu_*^{-1} (\nabla_\xi \times \boldsymbol{A}_\Delta(\boldsymbol{\xi}) + \nabla \times \boldsymbol{A}_0(\alpha\boldsymbol{\xi} + \boldsymbol{z}))_j \, d\boldsymbol{\xi}\\
&\quad + (\boldsymbol{R}_d(\boldsymbol{x}))_i \qquad (20)
\end{aligned}$$

where $\nu := \sigma_*\mu_0\omega\alpha^2$ as in Section III-C. Thus, to ensure that both terms have the same power of α, we need $\nu := O(1)$. This restriction also appeared in the asymptotic expansion (11) and, consequently, one might be tempted to write $\boldsymbol{R}_d(\boldsymbol{x}) = O(\alpha^4)$. However, this is incorrect since, despite the substitution of the Taylor series expressions in (15), the integrands in $\boldsymbol{R}_d(\boldsymbol{x})$ still depend on $\boldsymbol{A}_\Delta$, which itself is a function of α, and consequently, we cannot say that the remainder is of the form $|\boldsymbol{R}_d| \le C\alpha^4$ with C independent of α. A different approach is required to achieve this rigorously, leading to the asymptotic expansion (11) [4], [23].

This article has been accepted for inclusion in a future issue of this journal. Content is final as presented, with the exception of pagination.

In summary, in this section, we have shown that, in order for (4) to be a meaningful approximation to $(\boldsymbol{H}_\alpha - \boldsymbol{H}_0)(\boldsymbol{x})$, we need $\boldsymbol{x}$ to be away from B_α, the object's material parameters to be such that $\nu = O(1)$ and both the object's size α and the residual $\boldsymbol{R}_d(\boldsymbol{x})$ need to be small. However, (4) is not, in general, the leading term in an asymptotic expansion of $(\boldsymbol{H}_\alpha - \boldsymbol{H}_0)(\boldsymbol{x})$ as $\alpha \to 0$. We address when $\boldsymbol{R}_d(\boldsymbol{x})$ is small in Section IV-B.

B. Validity of (8) and an Explicit Formula for $\mathcal{M}$

We consider first the case of an object in a uniform field $\boldsymbol{H}_0$ and then second the case of an object excited by a nonuniform field $\boldsymbol{H}_0(\boldsymbol{x})$.

1) Excitation by a Uniform Field: In the case of excitation by a uniform field $\boldsymbol{H}_0$, we construct $\boldsymbol{A}_0(\boldsymbol{y}) = \frac{1}{2}\mu_0 \boldsymbol{H}_0 \times (\boldsymbol{y} - \boldsymbol{z})$ such that $\nabla_y \times \boldsymbol{A}_0 = \mu_0 \boldsymbol{H}_0$. Then, if choose to write

$$\boldsymbol{A}_\Delta(\boldsymbol{\xi}) = \sum_{k=1}^{3} \frac{\tilde{\boldsymbol{A}}_{\Delta,k}(\boldsymbol{\xi})}{2} (\boldsymbol{B}_0)_k = \mu_0 \sum_{k=1}^{3} \frac{\tilde{\boldsymbol{A}}_{\Delta,k}(\boldsymbol{\xi})}{2} \boldsymbol{e}_k \cdot \boldsymbol{H}_0$$

where $\tilde{\boldsymbol{A}}_{\Delta,k}(\boldsymbol{\xi})$ is the solution of the transmission problem

$$\begin{aligned}
\nabla_\xi \times \mu_*^{-1} \nabla_\xi \times \tilde{\boldsymbol{A}}_{\Delta,k} &= \mathrm{i}\omega\sigma_*\alpha^2 \tilde{\boldsymbol{A}}_{\Delta,k} \\
&\quad + \mathrm{i}\omega\sigma_*\alpha^2 \boldsymbol{e}_k \times \boldsymbol{\xi} \quad \text{in } B && \text{(21a)}\\
\nabla_\xi \cdot \tilde{\boldsymbol{A}}_{\Delta,k} &= 0 \quad \text{in } B^c && \text{(21b)}\\
\nabla_\xi \times \mu_0^{-1} \nabla_\xi \times \tilde{\boldsymbol{A}}_{\Delta,k} &= \boldsymbol{0} \quad \text{in } B^c && \text{(21c)}\\
[\boldsymbol{n} \times \tilde{\boldsymbol{A}}_{\Delta,k}]_\Gamma &= \boldsymbol{0} \quad \text{on } \Gamma && \text{(21d)}\\
[\boldsymbol{n} \times \mu^{-1} \nabla_\xi \times \tilde{\boldsymbol{A}}_{\Delta,k}]_\Gamma &= -2[\mu^{-1}]_\Gamma \boldsymbol{n} \times \boldsymbol{e}_k \quad \text{on } \Gamma && \text{(21e)}\\
\tilde{\boldsymbol{A}}_{\Delta,k} &= O(|\boldsymbol{\xi}|^{-1}) \quad \text{as } |\boldsymbol{\xi}| \to \infty && \text{(21f)}
\end{aligned}$$

we find that (20) becomes

$$(\boldsymbol{H}_\alpha - \boldsymbol{H}_0)(\boldsymbol{x})_i = \left(\boldsymbol{D}_x^2 G(\boldsymbol{x}, \boldsymbol{z})\right)_{ij} (\mathcal{M})_{jk} (\boldsymbol{H}_0)_k + (\boldsymbol{R}_d(\boldsymbol{x}))_i. \tag{22}$$

The coefficients of $\mathcal{M}$ agree with those derived in [21] and the transmission problem for $\tilde{\boldsymbol{A}}_{\Delta,k}$ agrees that for $\boldsymbol{\theta}_k$ derived in [4]. Explicitly

$$\begin{aligned}
(\mathcal{M})_{jk} &= -(\mathcal{C})_{jk} + (\mathcal{N})_{jk} \\
&= \frac{\mathrm{i}\alpha^3 \nu}{4} \boldsymbol{e}_j \cdot \int_B \boldsymbol{\xi} \times (\tilde{\boldsymbol{A}}_{\Delta,k} + \boldsymbol{e}_k \times \boldsymbol{\xi}) d\boldsymbol{\xi} \\
&\quad + \alpha^3 \left(1 - \frac{\mu_0}{\mu_*}\right) \boldsymbol{e}_j \cdot \int_B \left(\frac{1}{2} \nabla_\xi \times \tilde{\boldsymbol{A}}_{\Delta,k} + \boldsymbol{e}_k\right) d\boldsymbol{\xi}
\end{aligned} \tag{23}$$

and, by comparison with (11), we have $\boldsymbol{R}_d(\boldsymbol{x}) = \boldsymbol{R}(\boldsymbol{x}) = O(\alpha^4)$.

In summary, in this section, we have shown that using the representation (8) in the dipole approximation (4) is a meaningful approximation, which coincides with the asymptotic expansion for $(\boldsymbol{H}_\alpha - \boldsymbol{H}_0)(\boldsymbol{x})$ as $\alpha \to 0$, provided that $\boldsymbol{x}$ is away from B_α, $\boldsymbol{H}_0$ is a uniform field, the object's material parameters are such that $\nu = O(1)$, and α is small. In this case, (21) and (23) provide explicit formulae for the MPT calculation, which agree with our previous formulae [21].

2) Excitation by Nonuniform Fields: In the case of excitation by a nonuniform field, a method of approximating $\boldsymbol{H}_0(\boldsymbol{y})$ with $\boldsymbol{y}$ in B_α is required. Possible choices might include

$$\boldsymbol{H}_0|_{B_\alpha} \equiv \frac{1}{|B_\alpha|} \int_{B_\alpha} \boldsymbol{H}_0(\boldsymbol{y}) d\boldsymbol{y} \quad \text{or } \boldsymbol{H}_0|_{B_\alpha} \equiv \boldsymbol{H}_0(\boldsymbol{z}) \tag{24}$$

but it is unclear from the electrical engineering literature how $\boldsymbol{H}_0(\boldsymbol{y})$ should be averaged over B_α. In the applied mathematics community, $\boldsymbol{H}_0(\boldsymbol{y})$ is required to be analytic for $\boldsymbol{y}$ in B_α and is expanded using the Taylor series expansion

$$\begin{aligned}
(\boldsymbol{H}_0(\boldsymbol{y}))_i &= (\boldsymbol{H}_0(\alpha\boldsymbol{\xi} + \boldsymbol{z}))_i \\
&= (\boldsymbol{H}_0(\boldsymbol{z}))_i + \alpha(\boldsymbol{D}_z \boldsymbol{H}_0(\boldsymbol{z}))_{ij} (\boldsymbol{\xi})_j + O(\alpha^2)
\end{aligned} \tag{25}$$

as $\alpha \to 0$. It also follows from an uncurling formula [23] that a vector field $\boldsymbol{A}_0(\boldsymbol{y})$ that satisfies $\boldsymbol{H}_0(\boldsymbol{y}) = \mu_0^{-1} \nabla_y \times \boldsymbol{A}_0(\boldsymbol{y})$ is:

$$\begin{aligned}
(\boldsymbol{A}_0(\boldsymbol{y}))_i &= (\boldsymbol{A}_0(\alpha\boldsymbol{\xi} + \boldsymbol{z}))_i \\
&= \frac{\alpha\mu_0}{2} (\boldsymbol{H}_0(\boldsymbol{z}) \times \boldsymbol{\xi})_i \\
&\quad + \frac{\alpha^2 \mu_0}{3} (\boldsymbol{D}_z \boldsymbol{H}_0(\boldsymbol{z}))_{kj} (\boldsymbol{\xi})_j (\boldsymbol{e}_k \times \boldsymbol{\xi})_i \\
&\quad + O(\alpha^3)
\end{aligned} \tag{26}$$

as $\alpha \to 0$. But, even if the leading order terms in (25) and (26) are used in (19) to produce the transmission problem for $\tilde{\boldsymbol{A}}_\Delta \approx \boldsymbol{A}_\Delta$ as

$$\begin{aligned}
\nabla_\xi \times \mu_*^{-1} \nabla_\xi \times \tilde{\boldsymbol{A}}_\Delta &= \mathrm{i}\omega\sigma_*\alpha^2 \tilde{\boldsymbol{A}}_\Delta + \frac{\mathrm{i}\omega\sigma_*\alpha^2\mu_0}{2} \\
&\quad \boldsymbol{H}_0(\boldsymbol{z}) \times \boldsymbol{\xi} \quad \text{in } B && \text{(27a)}\\
\nabla_\xi \cdot \tilde{\boldsymbol{A}}_\Delta &= 0 \quad \text{in } B^c && \\
\nabla_\xi \times \mu_0^{-1} \nabla_\xi \times \tilde{\boldsymbol{A}}_\Delta &= \boldsymbol{0} \quad \text{in } B^c && \text{(27b)}\\
[\boldsymbol{n} \times \tilde{\boldsymbol{A}}_\Delta]_\Gamma &= \boldsymbol{0} \quad \text{on } \Gamma && \text{(27c)}\\
[\boldsymbol{n} \times \mu^{-1} \nabla_\xi \times \tilde{\boldsymbol{A}}_\Delta]_\Gamma &= -\mu_0 [\mu^{-1}]_\Gamma \boldsymbol{n} \times \boldsymbol{H}_0(\boldsymbol{z}) \quad \text{on } \Gamma && \text{(27d)}\\
\tilde{\boldsymbol{A}}_\Delta &= O(|\boldsymbol{\xi}|^{-1}) \quad \text{as } |\boldsymbol{\xi}| \to \infty && \text{(27e)}
\end{aligned}$$

it is not possible to rigorously say that $\boldsymbol{A}_\Delta = \tilde{\boldsymbol{A}}_\Delta + O(\alpha)$, and consequently, (16) still does not lead to an asymptotic expansion as $\alpha \to 0$. Instead, an alternative treatment is required to derive an asymptotic expansion for $(\boldsymbol{H}_\alpha - \boldsymbol{H}_0)(\boldsymbol{x})$ as $\alpha \to 0$ from (10) [4], [21]. Nonetheless, by further writing

$$\boldsymbol{A}_\Delta \approx \tilde{\boldsymbol{A}}_\Delta = \sum_{k=1}^{3} \frac{\tilde{\boldsymbol{A}}_{\Delta,k}}{2} (\boldsymbol{B}_0(\boldsymbol{z}))_k = \mu_0 \sum_{k=1}^{3} \frac{\tilde{\boldsymbol{A}}_{\Delta,k}}{2} \boldsymbol{e}_k \cdot \boldsymbol{H}_0(\boldsymbol{z})$$

and using (26) in (16), we find that $\tilde{\boldsymbol{A}}_{\Delta,k}$ solves the transmission problem in (21), and (20) becomes

$$(\boldsymbol{H}_\alpha - \boldsymbol{H}_0)(\boldsymbol{x})_i = \left(\boldsymbol{D}_x^2 G(\boldsymbol{x}, \boldsymbol{z})\right)_{ij} (\mathcal{M})_{jk} (\boldsymbol{H}_0(\boldsymbol{z}))_k + (\boldsymbol{R}_d(\boldsymbol{x}))_i \tag{28}$$

where again the coefficients of $\mathcal{M}$ are given by (23). By comparison with (11), we again have $\boldsymbol{R}_d(\boldsymbol{x}) = \boldsymbol{R}(\boldsymbol{x}) = O(\alpha^4)$.

In summary, in this section, we have shown that using the representation (8) in the dipole approximation (4) is a meaningful approximation, which coincides with the asymptotic expansion for $(\boldsymbol{H}_\alpha - \boldsymbol{H}_0)(\boldsymbol{x})$ as $\alpha \to 0$, provided

This article has been accepted for inclusion in a future issue of this journal. Content is final as presented, with the exception of pagination.

that $\boldsymbol{x}$ is away from B_α, $\boldsymbol{H}_0$ is analytic in B_α, we choose $\boldsymbol{H}_0|_{B_\alpha} = \boldsymbol{H}_0(\boldsymbol{z})$, the object's material parameters are such that $\nu = O(1)$, and α is small. In this case, (21) and (23) provide explicit formulae for the MPT calculation, which agree with our previous formulae [21].

V. Application of the Asymptotic Formula (11) to Realistic Scenarios

We have shown that the dipole expansion (4) agrees with the asymptotic expansion (11) for $(\boldsymbol{H}_\alpha - \boldsymbol{H}_0)(\boldsymbol{x})$ as $\alpha \to 0$ for both uniform and nonuniform background fields provided that $\boldsymbol{x}$ is away from B_α, $\nu = O(1)$, $\boldsymbol{H}_0$ is analytic in B_α, and we choose $\boldsymbol{H}_0|_{B_\alpha} = \boldsymbol{H}_0(\boldsymbol{z})$. The advantage of (11) is that we have a measure of its accuracy and an explicit formula for the MPT. We now show how (11) can be applied to practical situations.

A. Illustration of an MPT Computation

A finite-element computational procedure for solving (21), and computing the coefficients of $\mathcal{M}$, has been previously described in [21] and numerical results have been presented for a range of simply and multiply connected objects in [22], where excellent agreement with analytical and experimental results has been exhibited. As a further illustration of the validity of the approach, we consider a sphere of radius $\alpha = 0.01$ m, conductivity $\sigma_* = 5.96 \times 10^7$ S/m, and permeability $\mu_* = 1.5\mu_0$ and consider frequencies ranging from $f = 0.01$ Hz to $f = 1 \times 10^6$ Hz. The agreement between the numerical computation of the coefficients of $\mathcal{M}$, obtained by solving (21) using finite elements and applying (23) to compute $(\mathcal{M})_{jk}$, and the analytical solution given by (9) is shown in Fig. 2. The converged finite-element solution employs a discretization using order $p = 5$ elements and an unstructured mesh of 2425 tetrahedra and the figure shows that the agreement with the analytical solution is excellent for the range of frequencies considered. Note that by restricting the frequency range to $1 < f < 1000$ Hz, the skin depth becomes larger, and accurate solutions can already be obtained with lower order elements. The use of higher fidelity discretizations (higher elements and/or finer meshes close to the object's surface) is required for frequencies above 1000 Hz due to the need to resolve very thin skin depths at such frequencies.

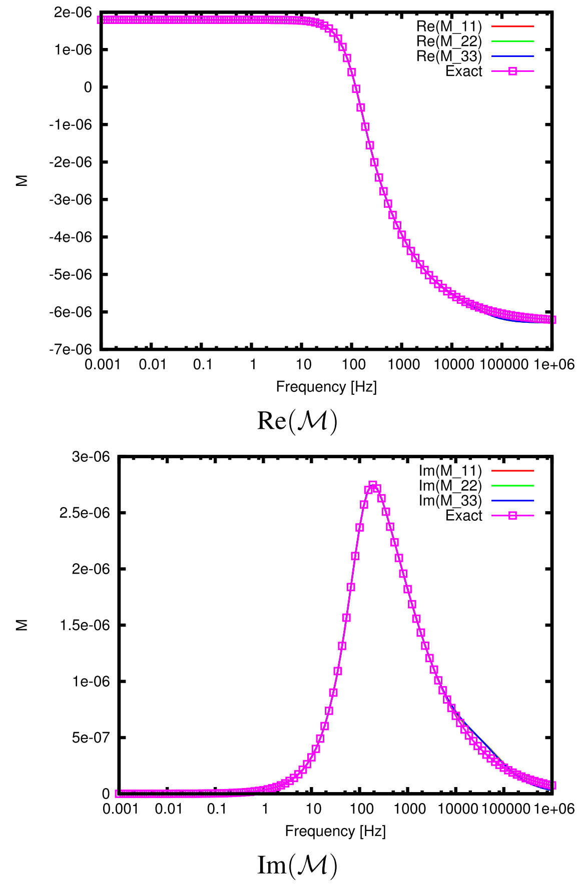

Fig. 2. Illustration of an MPT computation. Conducting permeable sphere of radius $\alpha = 0.01$ m with $\sigma_* = 5.96 \times 10^7$ S/m and $\mu_* = 1.5\mu_0$.

B. Object Placed in Background Field Generated by a Coil

As a first application of the asymptotic formula (11), we consider an object placed in the background field generated by an infinitely thin coil of radius a, with its center at position $\boldsymbol{y}$ and carrying a uniform current I^e. If the radius of the coil is such that $a \ll r = |\boldsymbol{z} - \boldsymbol{y}|$, i.e., the coil's radius is small compared with its distance from the object's center, then the background field at $\boldsymbol{z}$ can be approximated as

$$\begin{aligned}(\boldsymbol{H}_0(\boldsymbol{z}))_i &= \left(\boldsymbol{D}_z^2 G(\boldsymbol{z},\boldsymbol{y})\right)_{ij}\left(\boldsymbol{m}_0^e\right)_j \\ &= \left(\boldsymbol{D}_y^2 G(\boldsymbol{z},\boldsymbol{y})\right)_{ij}\left(\boldsymbol{m}_0^e\right)_j, \quad \left|\boldsymbol{m}_0^e\right| = I^e A^e \end{aligned} \tag{29}$$

where $A^e = \pi a^2$ and the orientation of the dipole moment $\boldsymbol{m}_0^e$ is chosen to be perpendicular to the coil's plane. If the origin is chosen to be at the center of the coil (i.e., $\boldsymbol{y} = \boldsymbol{0}$), we set $\tilde{\boldsymbol{r}} = -\boldsymbol{r}$ to be the coordinate measured from the coil's center and choose $\boldsymbol{m}_0 \parallel \boldsymbol{e}_3$, then (29) can be shown to reduce, in the spherical coordinates $(\tilde{r}, \tilde{\phi}, \tilde{\theta})$, to the familiar expressions $H_{\tilde{r}0} = (2\ I^e A^e/\tilde{r}^3)\cos\tilde{\theta}$, $H_{\tilde{\theta}0} = (I^e A^e/\tilde{r}^3)\sin\tilde{\theta}$, and $H_{\tilde{\phi}0} = 0$ found in many textbooks [19].

We now use (11) to replicate the situation described in [41], which consists of a sphere placed in the background field described by (29). We choose the coil to be located at position $\boldsymbol{y} = y_1\boldsymbol{e}_1 + y_2\boldsymbol{e}_2 + y_3\boldsymbol{e}_3$ and have a dipole moment $\boldsymbol{m}_0^e = I^e A^e \boldsymbol{e}_3$ and the object B_α to be located at $\boldsymbol{z} = \boldsymbol{0}$, as shown in Fig. 3, so that

$$\boldsymbol{H}_0(\boldsymbol{0}) = \frac{3I^e A^e}{4\pi|\boldsymbol{y}|^5}\begin{pmatrix} y_1 y_3 \\ y_2 y_3 \\ y_3^2 \end{pmatrix} - \frac{I^e A^e}{4\pi|\boldsymbol{y}|^3}\begin{pmatrix} 0 \\ 0 \\ 1 \end{pmatrix}. \tag{30}$$

In the case that B_α is a sphere of radius α, then

$$\mathcal{M}\boldsymbol{H}_0(\boldsymbol{0}) = \frac{3I^e A^e \overline{M}}{4\pi|\boldsymbol{y}|^5}\begin{pmatrix} y_1 y_3 \\ y_2 y_3 \\ y_3^2 \end{pmatrix} - \frac{I^e A^e \overline{M}}{4\pi|\boldsymbol{y}|^3}\begin{pmatrix} 0 \\ 0 \\ 1 \end{pmatrix}. \tag{31}$$

Wait [41] additionally chooses $y_2 = 0$ and, for this case, $\mathcal{M}\boldsymbol{H}_0(\boldsymbol{0}) = (p, 0, q)^T$, where

$$p = \frac{3I^e A^e y_1 y_3 \alpha^3 \overline{M}}{4\pi|\boldsymbol{y}|^3}, \quad q = \frac{I^e A^e \overline{M}}{4\pi|\boldsymbol{y}|^3}\left(\frac{3y_3^2}{|\boldsymbol{y}|^2} - 1\right) \tag{32}$$

This article has been accepted for inclusion in a future issue of this journal. Content is final as presented, with the exception of pagination.

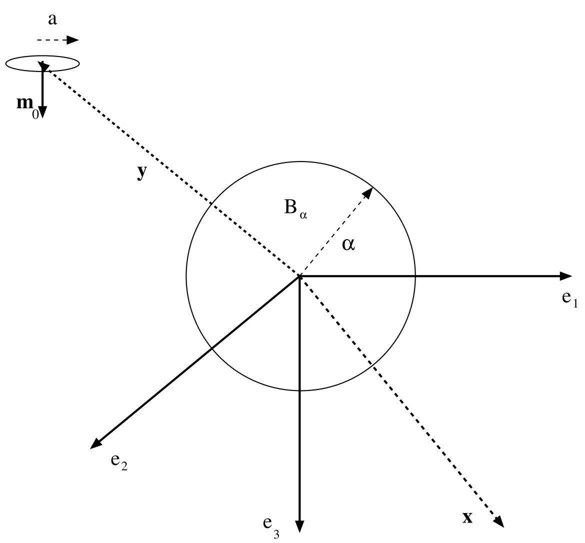

Fig. 3. Object placed in background field generated by a coil. Illustration of a conducting object B_α and a small coil idealized as a dipole.

which agree with the results.[6] It then follows from (11) that:

$$(\boldsymbol{H}_\alpha - \boldsymbol{H}_0)(\boldsymbol{x}) = \frac{1}{4\pi|\boldsymbol{x}|^3}\begin{pmatrix} p\left(\frac{3x_1^2}{|\boldsymbol{x}|^2}-1\right)+\frac{3x_1z_1q}{|\boldsymbol{x}|^2} \\ \frac{3x_1x_2p}{|\boldsymbol{x}|^2}+\frac{3x_2x_3q}{|\boldsymbol{x}|^2} \\ \frac{3x_1x_3p}{|\boldsymbol{x}|^2}+q\left(\frac{3x_3^2}{|\boldsymbol{x}|^2}-1\right)\end{pmatrix} + \boldsymbol{R}(\boldsymbol{x}) \tag{33}$$

where the first term matches the expression in [41].[7] For other shapes and other excitations, we can compute the coefficients of $\mathcal{M}$ numerically by solving (21) and then applying (23). Thus, we can similarly predict $(\boldsymbol{H}_\alpha - \boldsymbol{H}_0)(\boldsymbol{x})$ for other objects excited by a background field generated by a small coil.

C. Voltage Induced in a Small Coil

As a second application of asymptotic formula (11), we consider the problem of determining the voltage induced in a small coil due to the presence of a conducting permeable object. To do this, we recall the Lorentz reciprocity theorem, which states for a pair of current sources, $\boldsymbol{J}_0^e$ and $\boldsymbol{J}_0^m$, that

$$\int_{\mathbb{R}^3} \boldsymbol{J}_0^e \cdot \boldsymbol{E}^e d\boldsymbol{x} = \int_{\mathbb{R}^3} \boldsymbol{J}_0^m \cdot \boldsymbol{E}^m d\boldsymbol{x}. \tag{34}$$

Labeling e as the emitter and m as the receiver, this states that the response is unchanged if the sources are interchanged. In reality, $\boldsymbol{J}_0^e$ and $\boldsymbol{J}_0^m$ have small support, which are only nonzero in the coils. Assuming that the emitting and receiver coils are centered at $\boldsymbol{y}$ and $\boldsymbol{x}$, respectively, using a Taylor series approximation about the center of the current sources, for small coils, choosing $\boldsymbol{J}_0^m$ so that it is orientated in the direction of the measurement coil, and applying (11), we have shown in [22] that (34) coincides with the voltage induced in the receiver coil by the presence of B_α and simplifies to

$$\begin{aligned} V^{\text{ind}} &\approx C\left(\boldsymbol{m}_0^m\right)_i \left(\boldsymbol{D}_x^2 G(\boldsymbol{x},\boldsymbol{z})\right)_{ij} (\mathcal{M})_{jk} \left(\boldsymbol{H}_0^e(\boldsymbol{z})\right)_k \\ &= C\boldsymbol{H}_0^m(\boldsymbol{z}) \cdot \left(\mathcal{M}\boldsymbol{H}_0^e(\boldsymbol{z})\right). \end{aligned} \tag{35}$$

This expression assumes that both coils can be treated as dipole sources with their radii being small compared with their distance from the object, and consequently, we choose $\boldsymbol{H}_0^e(\boldsymbol{z})$ to be given by (29). We also construct $\boldsymbol{H}_0^m(\boldsymbol{z})$ in a similar way where we assume that $|\boldsymbol{m}_0^m| = A^m I^m$, where A^m is the area of the measurement coil and I^m is the current that would flow, if it was an exciter, and its orientation to be perpendicular to the plane of the measurement coil. To ensure that V^{ind} has units of volts, we set $C = -\mathrm{i}\omega\mu_0/I^m$ and then we find that

$$V^{\text{ind}} = -\frac{\mathrm{i}\omega\mu_0}{I^m}\boldsymbol{H}_0^m(\boldsymbol{z}) \cdot \left(\mathcal{M}\boldsymbol{H}_0^e(\boldsymbol{z})\right) \tag{36}$$

and this is then consistent with [1], [28], and [46]. Note that our result is the complex conjugate of theirs due to their assumption of $e^{\mathrm{i}\omega t}$ rather than $e^{-\mathrm{i}\omega t}$ assumed here.

D. Voltage Induced in Solenoids

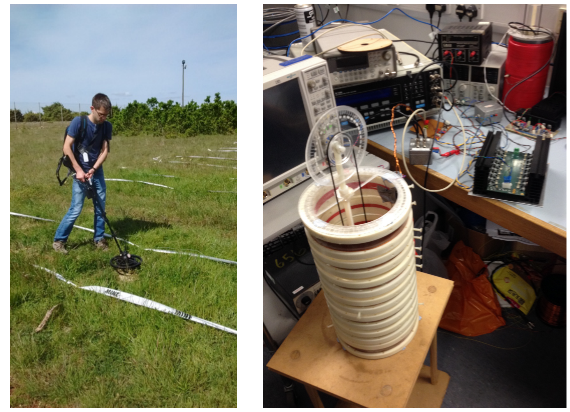

Fig. 4. Voltage in solenoids. (Left) Photograph showing metal detection using the MPT for characterization [16]. (Right) Photograph showing the experimental setup proposed in [33] for determining MPT coefficients.

As a third application of asymptotic formula (11), we determine the voltage induced in a coil, whose dimensions are not small compared with the size of the object when the background field is also generated by a larger coil. In such cases, the background magnetic field cannot be approximated by a dipole source with constant dipole moment. Experimental studies have shown that the induced voltage induced in larger coils, including shorter solenoids, used in-line metal detectors [44] and landmine detection [16], and solenoids whose length is large compared with their diameter [33], as shown in Fig. 4, takes the same form as given in (36). We now show that this is indeed the case.

The background field $\boldsymbol{H}_0(\boldsymbol{z}) = \boldsymbol{H}_0^e(\boldsymbol{z})$ generated by an exciter for a general current distribution $\boldsymbol{J}_0^e$ can be calculated for a general current distribution using the Biot–Savart law

$$\boldsymbol{H}_0^e(\boldsymbol{z}) = \int_{\text{supp }\left(\boldsymbol{J}_0^e\right)} \frac{\boldsymbol{J}_0^e \times (\boldsymbol{z}-\boldsymbol{x})}{4\pi|\boldsymbol{z}-\boldsymbol{x}|^3} d\boldsymbol{x}. \tag{37}$$

[6] Note that in Wait's [41] notation, $b \equiv \alpha$, $-x_1 \equiv y_1$, $-z_1 \equiv y_3$, and $r_1 \equiv |\boldsymbol{y}|$, and R_1 that he defines in his (22) is equivalent to $-M/(2\pi\alpha^3)$ in this paper. His solution for p and q is out by a factor of π. To correct Wait's expression for p and q in his (32), they should be multiplied by π and they then match our (32).

[7] Note that in Wait's notation $x_0 \equiv x_1$, $y_0 \equiv x_2$, $x_3 \equiv x_3$, and $r_0 \equiv |\boldsymbol{x}|$, also the expression presented by Wait [41] has an error in the third component, which has been corrected in (33).

This article has been accepted for inclusion in a future issue of this journal. Content is final as presented, with the exception of pagination.

In the case of an exciting solenoid of length L^e, radius R^e with N^e turns wound anticlockwise each carrying current I^e with the origin placed at the center of solenoid, as shown in Fig. 5(a), and it can be shown [38] for $\boldsymbol{z} = z_3\boldsymbol{e}_3$ that

$$\boldsymbol{H}_0^e(\boldsymbol{z}) = \frac{N^e I^e}{2L^e}\left(\frac{\frac{L^e}{2R^e} - \frac{z_3}{R^e}}{\sqrt{1+\left(\frac{L^e}{2R^e} - \frac{z_3}{R^e}\right)^2}} + \frac{\frac{L^e}{2R^e} + \frac{z_3}{R^e}}{\sqrt{1+\left(\frac{L^e}{2R^e} + \frac{z_3}{R^e}\right)^2}}\right)\boldsymbol{e}_3. \quad (38)$$

If the object is positioned such that $z_3 \ll L^e/2$, then the background field at this location simplifies to

$$\boldsymbol{H}_0^e(\boldsymbol{z}) = \frac{N^e I^e}{L^e}\left(\frac{\frac{L^e}{2R^e}}{\sqrt{1+\left(\frac{L^e}{2R^e}\right)^2}}\right)\boldsymbol{e}_3 \quad (39)$$

and for a long solenoid, with $L^e/(2R^e) \gg 1$, this simplifies further to $\boldsymbol{H}_0^e(\boldsymbol{z}) = (N^e I^e/L^e)\boldsymbol{e}_3$.

The voltage induced in a single turn of a measurement solenoid, shown in Fig. 5(b), is given by

$$V^{\text{ind}} = \int_C (\boldsymbol{E}_\alpha - \boldsymbol{E}_0)(\boldsymbol{x})\cdot\boldsymbol{\tau}\, d\boldsymbol{x} = \int_S \nabla\times(\boldsymbol{E}_\alpha - \boldsymbol{E}_0)(\boldsymbol{x})\cdot\boldsymbol{n}\, d\boldsymbol{x}$$

where the solenoid has been placed so that it is centered about the origin, $C = \partial S$ defines a loop of the measurement solenoid, $\boldsymbol{\tau}$ is the unit tangent to C, and $S := \{(\rho,\phi) : 0 \le \rho \le R^m, 0 \le \phi \le 2\pi\}$ is the surface enclosed by C. As mentioned above, we particularize this to the case where the object is placed at $\boldsymbol{z} = z_3\boldsymbol{e}_3$, substitute the leading order term in (11), and find that for a clockwise winding[8]

$$\begin{aligned} V^{\text{ind}} &\approx \mathrm{i}\omega\mu_0 \int_S \boldsymbol{n}\cdot(\boldsymbol{H}_\alpha - \boldsymbol{H}_0)(\boldsymbol{x})d\boldsymbol{x} \\ &\approx -\mathrm{i}\omega\mu_0 \int_S \left(\boldsymbol{D}_x^2 G(\boldsymbol{x}, z_3\boldsymbol{e}_3)\right)_{3j} d\boldsymbol{x} (\mathcal{M})_{jk}\left(\boldsymbol{H}_0^e(\boldsymbol{z})\right)_k. \end{aligned}$$

The measurement solenoid is of length L^m, and hence, to find the total induced voltage, we find, after evaluating $(\boldsymbol{D}_x^2 G(\boldsymbol{x}, z_3\boldsymbol{e}_3))_{3j}\boldsymbol{e}_j$, that we need to compute the integral given in (40) (see next page) where $x_1 = \rho\cos\phi$ and $x_2 = \rho\sin\phi$ and the substitution $u = x_3 - z_3$ has been made. By performing the integration with respect to ϕ, ρ, and u, in turn, we find that

$$\begin{aligned} \mathrm{I} &= \frac{1}{L^m}\int_{-\frac{L^m}{2}-z_3}^{\frac{L^m}{2}-z_3}\int_0^{R^m}\left(\frac{3\rho u^2}{2(\rho^2+u^2)^{5/2}} - \frac{\rho}{2(\rho^2+u^2)^{3/2}}\right) d\rho\, du\,\boldsymbol{e}_3 \\ &= \frac{1}{2L^m}\int_{-\frac{L^m}{2}-z_3}^{\frac{L^m}{2}-z_3}\left(\frac{1}{\sqrt{(R^m)^2+u^2}} - \frac{u^2}{((R^m)^2+u^2)^{3/2}}\right) du\,\boldsymbol{e}_3 \\ &= \frac{1}{2L^m}\left(\frac{\frac{L^m}{2R^m} - \frac{z_3}{R^m}}{\sqrt{1+\left(\frac{L^m}{2R^m} - \frac{z_3}{R^m}\right)^2}} + \frac{\frac{L^m}{2R^m} + \frac{z_3}{R^m}}{\sqrt{1+\left(\frac{L^m}{2R^m} + \frac{z_3}{R^m}\right)^2}}\right)\boldsymbol{e}_3 \end{aligned}$$

[8]Note the asymptotic formula is only valid for $\boldsymbol{x}$ exterior to the object but, assuming B_α to be small, we apply it over the complete surface even though the surface may intersect B_α if a small object is placed inside a solenoid.

which has a similar form in (38) and can be simplified for locations $z_3 \ll L_m/2$ and solenoids with $L_m/(2R_m) \gg 1$. Thus, in general, we find that the induced voltage in a measurement solenoid with N^m turns will have the form

$$V^{\text{ind}} = -\frac{\mathrm{i}\omega\mu_0}{I^m N^m}\boldsymbol{H}_0^m(\boldsymbol{z})\cdot\left(\mathcal{M}\boldsymbol{H}_0^e(\boldsymbol{z})\right) \quad (41)$$

where, in general, both $\boldsymbol{H}_0^e(\boldsymbol{z})$ and $\boldsymbol{H}_0^m(\boldsymbol{z})$ are nonuniform. For the situation described above where $\boldsymbol{z} = z_3\boldsymbol{e}_3$, the fields satisfy $\boldsymbol{H}_0^e(\boldsymbol{z}) \parallel \boldsymbol{e}_3$, $\boldsymbol{H}_0^m(\boldsymbol{z}) \parallel \boldsymbol{e}_3$ and become uniform provided that $z_3 \ll L^e/2$, $z_3 \ll L^m/2$.

If the object is rotated (as is possible using the experimental setup described in [33]), then the components of $\mathcal{M}$ transform as

$$(\mathcal{M}')_{ij} = (R)_{ik}(R)_{j\ell}(\mathcal{M})_{k\ell}. \quad (42)$$

For example, for a rotation β about the axis associated with $\boldsymbol{e}_2$, the orthogonal matrix R is

$$R = R^{\boldsymbol{e}_2}(\beta) = \begin{pmatrix} \cos\beta & 0 & \sin\beta \\ 0 & 1 & 0 \\ -\sin\beta & 0 & \cos\beta \end{pmatrix}.$$

Then, by replacing $\mathcal{M}$ by $\mathcal{M}'$ in (41) and performing suitable rotations (see Section V-E), the voltage V^{ind} can be used to deduce the components of the MPT [22], [33]. In [22], we have shown how the coefficients of $\mathcal{M}$ for a Remington rifle cartridge transform when the object is rotated about $\boldsymbol{e}_2$ and our numerical results agree well with the experimental measurements performed for the same object shown in [33].

E. Measuring a Tensor's Rank

We have seen how the rank 2 MPT characterizes the shape and material properties of an object and appears as $\mathcal{M}$ in the leading order term of an asymptotic expansion as the size of the object tends to zero (11). However, $\mathcal{M}$ only provides limited information about an object, and to be able to better characterize an object's shape and material parameters, higher order terms should be used. Such information can be captured by using the complete asymptotic expansion proposed in [23] and using the higher rank GMPTs (with the rank 2 MPT being the simplest case) for describing an object's characteristics. In practice, one would like to determine the maximum rank of tensor that is required to describe the data.

To fix ideas, we consider a hypothetical measurement system, similar to that described in [33], with fixed exciting and measurement coils and the ability to rotate the object. In this system, we envisage that the coils are shorter than the long solenoids in [33] and/or that the object is placed at the ends of the coils so that $\boldsymbol{H}_0^e(\boldsymbol{z})$ and $\boldsymbol{H}_0^m(\boldsymbol{z})$ are nonuniform. We choose to rotate the object about each of the axes associated with $\boldsymbol{e}_1$, $\boldsymbol{e}_2$, and $\boldsymbol{e}_3$, in turn,[9] and, for a rotation θ, in the list (α,β,γ), about the considered axis, the induced voltage will be $V^{\text{ind}}(\theta)$. If the induced voltage can be described by a rank 2 tensor then (41) applies, although a

[9]Another possibility is to perform simultaneous rotation about $\boldsymbol{e}_1$, $\boldsymbol{e}_2$, and $\boldsymbol{e}_3$, and in this case $(R(\alpha,\beta,\gamma))_{ij} = (R^{\boldsymbol{e}_1}(\alpha))_{ik}(R^{\boldsymbol{e}_2}(\beta))_{k\ell}(R^{\boldsymbol{e}_3}(\gamma))_{\ell j}$, where $R^{\boldsymbol{e}_1}(\alpha)$, $R^{\boldsymbol{e}_2}(\beta)$, and $R^{\boldsymbol{e}_3}(\gamma)$ are the rotation matrices and α, β, and γ are the the rotation angles. The described approach can be easily extended to the case of simultaneous rotation $\theta = \alpha = \beta = \gamma$.

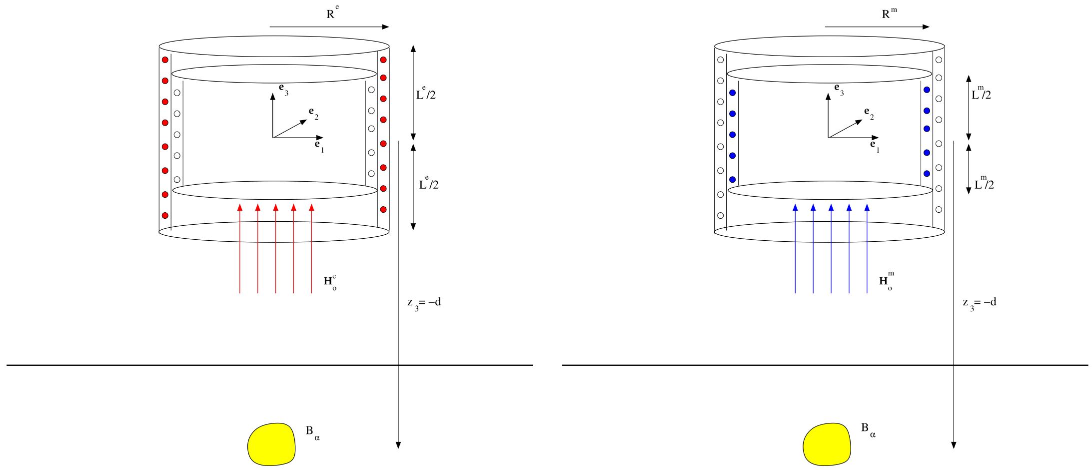

Fig. 5. Voltage in solenoids. Diagrams illustrating the conducting object B_α and a possible position exterior to (Left) exciting solenoid and (Right) measurement solenoid.

more precise description would relate V^{ind} to the GMPT coefficients. As the object is rotated, the coefficients of the MPT transform according to (42) with similar results holding for the transformation of the higher rank GMPTs [23]. Thus, $V^{\text{ind}}(\theta)$ can be expressed in terms of the coefficients of the MPT/GMPTs (for the object's original configuration) and products of cosines and sines of θ. In general, the highest powers of these trigonometric functions in a transformed rank K tensor will be K. For example, for $K=2$, $V^{\text{ind}}(\theta)$ will be the function of the coefficients of $\mathcal{M}'$, which, in turn, can be expressed in terms of the linear combinations of $\cos^2\theta$ and $\sin^2\theta$ as well as lower order powers and products of $\cos\theta$ and $\sin\theta$. The coefficients of these linear combinations involve the coefficients of $\mathcal{M}$, which are independent of the rotation.

We recall that $\cos^K\theta$ can be written as a linear combination of cosines of multiple angles $\cos K\theta$, $\cos(K-1)\theta, \dots,$ and $\cos 0$, which we write as $\cos^K(\theta) = \text{span}\{\cos K\theta, \cos(K-1)\theta, \dots \cos 0\}$. Similarly, $\sin^K\theta = \text{span}\{\sin K\theta, \sin(K-1)\theta, \dots \sin\theta\}$ if K is odd and $\sin^K\theta = \text{span}\{\cos K\theta, \cos(K-1)\theta, \dots \cos 0\}$ if K is even. Using these properties, we can deduce that the Fourier series

$$f(\theta) = \sum_{n=-\infty}^{\infty} c_n e^{\text{i}n\theta}, \quad c_n = \frac{1}{2\pi}\int_0^{2\pi} f(\theta)e^{-\text{i}n\theta}d\theta \tag{43}$$

applied to $f(\theta) = V^{\text{ind}}(\theta)$ reduces to the finite sum

$$f(\theta) = \sum_{n=-K}^{K} c_n e^{\text{i}n\theta} \tag{44}$$

using knowledge of the integrals of products of trigonometric functions.

To determine the rank of tensor that best fits the measured data, we determine the maximum K needed to fit the data. We note that the induced voltage $f(\theta) = V^{\text{ind}}(\theta)$ is a periodic function satisfying $f(\theta) = f(\theta+2\pi)$ as the object is rotated; therefore, for efficiency, we apply a discrete Fourier transform (DFT). We choose an even integer number N, select candidate rotations as $\theta_k = 2\pi k/N$, $k = 0,\dots,N-1$, and for each rotation, measure the induced voltage $f_k = V_k^{\text{meas}} = f(\theta_k)$, $k = 0,\dots,N-1$. By setting $f_N := (f_0, f_1, \dots, f_{N-1})^T$, $(W)_{kn} := e^{-2\pi\text{i}(k-1)(n-1)/N}$, $k,n = 1,\dots,N$ and applying

$$\tilde{c}^N = \frac{1}{N} W f^N \tag{45}$$

we obtain $\tilde{c}^N := (\tilde{c}_0, \tilde{c}_1, \dots, \tilde{c}_{N-1})^T$, which are the approximate Fourier coefficients. Due to periodicity, we recall that $\tilde{c}_k = \tilde{c}_{k-N}$ and $f_k = f_{k-N}$. This means that the DFT provides the trigonometric polynomial

$$p(\theta) = \sum_{n=-N/2+1}^{N/2-1} \tilde{c}_n e^{\text{i}n\theta} + \tilde{c}_{N/2}\cos\frac{N}{2}\theta \tag{46}$$

which satisfies $p(\theta_k) = f(\theta_k) = f_k = V_k^{\text{ind}}$ for $k = 0,\dots,N-1$, and for the case of $\tilde{c}_{N/2} = 0$, reduces to (44) with $K = N/2-1$. To check if we have not been lucky with the choice of θ_k, we use the criteria

$$\left| V^{\text{meas}}(\theta) - \sum_{n=-K}^{K} \tilde{c}_n e^{\text{i}n\theta} \right| < \varepsilon \tag{47}$$

where ε is the measurement noise, for some $\theta \neq \theta_k$, k=0,$\dots$, $N-1$, to check if sufficient terms have been included. But, as $\tilde{c}_{N/2} = 0$ is not guaranteed, we should only

$$\begin{aligned}
\mathrm{I} &= \frac{1}{L^m}\int_{-\frac{L^m}{2}}^{\frac{L^m}{2}}\int_0^{R^m}\int_0^{2\pi}\left(\frac{3\rho}{4\pi(\rho^2+(x_3-z_3)^2)^{5/2}}\begin{pmatrix}\rho(x_3-z_3)\cos\phi\\ \rho(x_3-z_3)\sin\phi\\ (x_3-z_3)^2\end{pmatrix} - \frac{\rho}{4\pi(\rho^2+(x_3-z_3)^2)^{3/2}}\begin{pmatrix}0\\0\\1\end{pmatrix}\right)d\phi d\rho dx_3\\
&= \frac{1}{L^m}\int_{-L^m/2-z_3}^{L^m/2-z_3}\int_0^{R^m}\int_0^{2\pi}\left(\frac{3\rho}{4\pi(\rho^2+u^2)^{5/2}}\begin{pmatrix}\rho u\cos\phi\\ \rho u\sin\phi\\ u^2\end{pmatrix} - \frac{\rho}{4\pi(\rho^2+u^2)^{3/2}}\begin{pmatrix}0\\0\\1\end{pmatrix}\right)d\phi d\rho du
\end{aligned} \tag{40}$$

This article has been accepted for inclusion in a future issue of this journal. Content is final as presented, with the exception of pagination.

accept $K = N/2 - 1$ if both (47) and $\tilde{c}_{N/2} = 0$ are satisfied. We summarize the steps in Algorithm 1. We repeat the process for rotations about each axis and choose the rank of tensor to be the maximum K found from considering the three cases.

Algorithm 1 Algorithm for Determining the Rank of Tensor K Required to Represent a Given Set of Measured Data $f(\theta)$ Using DFT

Set $N = 2$ ▷ N must be even

while $\left| V^{\text{meas}}(\theta) - \sum_{n=-N/2+1}^{N/2-1} \tilde{c}_n e^{\text{i}n\theta} \right| \not< \varepsilon$ or $\tilde{c}_{N/2} \neq 0$ **do**

  $N = N + 2$

  Set $\theta_k = (2\pi k)/N$, $k = 0, \cdots, N-1$

  Measure $f_k = f(\theta_k)$ and set $f^N = (f_0, f_1, \cdots, f_{N-1})^T$

  Set W to be the $N \times N$ matrix with $(W)_{kn} = e^{-2\pi \text{i}(k-1)(n-1)/N}$, $k, n = 1, \cdots, N$

  Compute $\tilde{c}^N = \frac{1}{N} W f^N$ where $\tilde{c}^N = (\tilde{c}_0, \tilde{c}_1, \cdots, \tilde{c}_{N-1})^T$

  Set $\tilde{c}_{k-N} = \tilde{c}_k$, $k = 1, \cdots, N-1$

end while

$K = N/2 - 1$

Following the application of Algorithm 1, a data set consisting of $3N$ voltage measurements $V^{\text{meas}}(\theta_k)$ for $\theta_k = \alpha_k$, $\theta_k = \beta_k$, and $\theta_k = \gamma_k$, in turn, with $k = 1, \ldots, N$, is available, and potentially, this data set can also be used to determine the coefficients of the MPT (and GMPTs if $K > 2$). However, although this represents an overdetermined linear problem for the tensor coefficients, the considered rotations may not lead to a suitable set of directions for their computation. To illustrate this, consider $K = 2$ and choose fixed background fields orientated in the same direction, such that $\boldsymbol{H}_0^m(\boldsymbol{z}) = |\boldsymbol{H}_0^m(\boldsymbol{z})|\boldsymbol{u}$ and $\boldsymbol{H}_0^e(\boldsymbol{z}) = |\boldsymbol{H}_0^e(\boldsymbol{z})|\boldsymbol{u}$, then

$$\begin{aligned} V^{\text{ind}}(\theta_k) &= -\frac{\text{i}\omega\mu_0}{I^m N^M} \boldsymbol{H}_0^m(\boldsymbol{z}) \cdot \left(\mathcal{M}' \boldsymbol{H}_0^e(\boldsymbol{z})\right) \\ &= -\frac{\text{i}\omega\mu_0}{I^m N^M} \left|\boldsymbol{H}_0^m(\boldsymbol{z})\right| \left|\boldsymbol{H}_0^e(\boldsymbol{z})\right| \boldsymbol{v}^{[k]} \cdot (\mathcal{M}\boldsymbol{v}^{[k]}) \end{aligned} \quad (48)$$

where $\boldsymbol{v}^{[k]} = (\mathcal{R}(\theta_k)^T \boldsymbol{u}) = (\mathcal{R}(\theta_k))_{ji} (\boldsymbol{u})_j \boldsymbol{e}_i$ and we have, from the application of Algorithm 1, the measured data $V_k^{\text{meas}} \approx V^{\text{ind}}(\theta_k)$. Then, in order to determine the coefficients of a symmetric $\mathcal{M}$ from the data, there need to be, among $\boldsymbol{v}^{[k]}$, six independent directions that correspond to points on a projective space that do not lie on a projective conic [25].[10] This is equivalent to saying that $A^{[k]} := \boldsymbol{v}^{[k]} \otimes \boldsymbol{v}^{[k]}$ spans the space of symmetric rank 2 tensors. To check if the directions are suitable, the rank of the $3N \times 6$ real matrix B, whose kth row is of the form

$$(B)_{k1:6} := ((A^{[k]})_{11}\ (A^{[k]})_{12}\ (A^{[k]})_{13}\ (A^{[k]})_{22}\ (A^{[k]})_{23}\ (A^{[k]})_{33}) \quad (49)$$

can be computed. If $\text{rank}(B) = 6$, the directions can be used for determining $\mathcal{M}$, if not, additional directions $\boldsymbol{v}^{[k]}$ need to chosen, and rows added to B, until its rank is 6. Extensions are also possible for determining the suitability of candidate directions for computing the coefficients of higher rank tensors.

[10]Any five points define a projective conic; if the sixth also lies on the conic, this choice is invalid for determining the coefficients of $\mathcal{M}$.

VI. Conclusion

In this paper, we have emphasized the advantages provided by the asymptotic formula in (11) over the multipole expansion (4) for $(\boldsymbol{H}_\alpha - \boldsymbol{H}_0)(\boldsymbol{x})$ with $\boldsymbol{x}$ away from B_α, namely, that it provides a measure accuracy of the approximation and an explicit formula for the MPT in the form of $\mathcal{M}$, which holds for general objects. We have shown that (4) does coincide with (11) provided that the object is small and $\nu = O(1)$ and the background field $\boldsymbol{H}_0$ is either uniform or, for nonuniform excitations, that it is analytic in B_α. In both the cases, choosing $\boldsymbol{H}_0|_{B_\alpha} = \boldsymbol{H}_0(\boldsymbol{z})$, we find that (21) and (23) provide explicit formulae for the calculation of the MPT's coefficients, which agree with our previous formulae [21], thus justifying the approximation for time harmonic excitations by both uniform and nonuniform background fields and making explicit the situations in which it provides a good approximation. We have also presented a series of applications of the asymptotic formula (11) to realistic metal detection situations and described a procedure for predicting the rank of tensor required for describing a data set. Ammari *et al.* [3] have described how multifrequency voltage measurements are useful for object classification in a related electrosensing problem. Using an analogous approach for the metal detection problem offers considerable potential for object classification using (G)MPTs and we intend to report on this in a forthcoming work. We also intend, in the further forthcoming work, to justify the existence of an equivalent transient MPT representation and provide and explicit formulae for its calculation.

Appendix
Proof of (16)

On insertion of (15) into (12), we find that

$$(\boldsymbol{H}_\alpha - \boldsymbol{H}_0)(\boldsymbol{x})_i = \text{I}_1 - \text{I}_2 + \text{I}_3 + (\boldsymbol{R}_d(\boldsymbol{x}))_i \quad (50)$$

where, using Einstein summation convention,

$$\begin{aligned} \text{I}_1 &:= \text{i}\alpha^3 \sigma_* \omega \epsilon_{ijp} (\nabla_x G(\boldsymbol{x}, \boldsymbol{z}))_j \int_B (\boldsymbol{A}_\alpha(\alpha\boldsymbol{\xi} + \boldsymbol{z}))_p d\boldsymbol{\xi} \\ \text{I}_2 &:= \text{i}\alpha^4 \sigma_* \omega \epsilon_{ijp} \left(\boldsymbol{D}_x^2 G(\boldsymbol{x}, \boldsymbol{z})\right)_{jk} \int_B (\boldsymbol{\xi})_k (\boldsymbol{A}_\alpha(\alpha\boldsymbol{\xi} + \boldsymbol{z}))_p d\boldsymbol{\xi} \\ \text{I}_3 &:= \alpha^3 \left(\frac{\mu_*}{\mu_0} - 1\right) \left(\boldsymbol{D}_x^2 G(\boldsymbol{x}, \boldsymbol{z})\right)_{ij} \\ &\quad \int_B \mu_*^{-1} (\nabla \times \boldsymbol{A}_\alpha(\alpha\boldsymbol{\xi} + \boldsymbol{z}))_j d\boldsymbol{\xi} \end{aligned}$$

where ϵ_{ijk} is the standard alternating tensor, which satisfies

$$\epsilon_{ijk} = \begin{cases} +1 & \text{Even permutation of indices } 1, 2, 3 \\ -1 & \text{Odd permutation of indices } 1, 2, 3 \\ 0 & \text{Otherwise.} \end{cases}$$

With the exception of I_3, which is already of the correct form, we now consider the treatment of each term separately.

This article has been accepted for inclusion in a future issue of this journal. Content is final as presented, with the exception of pagination.

A. Consideration of I_1

In light of (10), it useful to rewrite I_1 in terms of an integral over B_α and then to transform to a surface integral. Application of transmission conditions then yields

$$\begin{aligned}\mathrm{I}_1 &= \epsilon_{ijp}(\nabla_x G(\boldsymbol{x},\boldsymbol{z}))_j \int_{B_\alpha} (\nabla_y \times (\boldsymbol{H}_\alpha(\boldsymbol{y}) - \boldsymbol{H}_0(\boldsymbol{y}))_p d\boldsymbol{y}\\ &= \epsilon_{ijp}(\nabla_x G(\boldsymbol{x},\boldsymbol{z}))_j \int_{\Gamma_\alpha} (\boldsymbol{n}^- \times (\boldsymbol{H}_\alpha(\boldsymbol{y}) - \boldsymbol{H}_0(\boldsymbol{y}))_p \Big|_- d\boldsymbol{y}\\ &= -\epsilon_{ijp}(\nabla_x G(\boldsymbol{x},\boldsymbol{z}))_j \int_{B_\alpha^c} (\nabla_y \times (\boldsymbol{H}_\alpha(\boldsymbol{y}) - \boldsymbol{H}_0(\boldsymbol{y}))_p d\boldsymbol{y}\\ &= 0 \end{aligned} \tag{51}$$

since $\nabla \times (\boldsymbol{H}_\alpha - \boldsymbol{H}_0) = \boldsymbol{0}$ in B_α^c for excitation by a uniform field and $\nabla \times (\boldsymbol{H}_\alpha - \boldsymbol{H}_0) = \boldsymbol{J}_0 - \boldsymbol{J}_0 = \boldsymbol{0}$ in B_α^c otherwise.

B. Consideration of I_2

We can rewrite I_2 as

$$\mathrm{I}_2 = \mathrm{i}\omega\sigma_*\epsilon_{ijp}\left(\boldsymbol{D}_x^2 G(\boldsymbol{x},\boldsymbol{z})\right)_{jk} \int_{B_\alpha} (\boldsymbol{y}-\boldsymbol{z})_k (\boldsymbol{A}_\alpha(\boldsymbol{y}))_p d\boldsymbol{y} \tag{52}$$

and to be able to take $\boldsymbol{D}_x^2 G(\boldsymbol{x},\boldsymbol{z})$ out of the cross product, we need some additional information. It is instructive to consider the integral

$$\mathrm{I}_4 := (\mathcal{Q})_{kp} = \int_{B_\alpha} (\boldsymbol{y}-\boldsymbol{z})_k (\boldsymbol{A}_\alpha(\boldsymbol{y}))_p d\boldsymbol{y}$$

which also represents the components of a rank 2 tensor $\mathcal{Q}$, and to express it in an alternative form by using the transmission problem (14). It follows that:

$$\begin{aligned}\mathrm{I}_4 &= \frac{1}{\mathrm{i}\omega\sigma_*}\int_{B_\alpha} ((\boldsymbol{y}-\boldsymbol{z})_k \boldsymbol{e}_p)\cdot \nabla_y \times \mu_*^{-1}\nabla_y \times \boldsymbol{A}_\alpha d\boldsymbol{y}\\ &= \frac{1}{\mathrm{i}\omega\sigma_*}\left(\int_{\Gamma_\alpha} \boldsymbol{n}^- \cdot \left(\mu_*^{-1}\nabla_y \times \boldsymbol{A}_\alpha \times ((\boldsymbol{y}-\boldsymbol{z})_k\boldsymbol{e}_p)\right)\Big|_- d\boldsymbol{y}\right.\\ &\qquad \left. - \int_{B_\alpha} \boldsymbol{e}_k \times \boldsymbol{e}_p \cdot \mu_*^{-1}\nabla_y \times \boldsymbol{A}_\alpha d\boldsymbol{y}\right)\end{aligned}$$

where we see that the latter term is skew symmetric with respect to k and p. Focusing on the first term, we find, by application of the transmission conditions in (14), that in the case of excitation by $\boldsymbol{J}_0$

$$\begin{aligned}&\int_{\Gamma_\alpha} \boldsymbol{n}^- \cdot \left(\mu_*^{-1}\nabla_y \times \boldsymbol{A}_\alpha \times ((\boldsymbol{y}-\boldsymbol{z})_k\boldsymbol{e}_p)\right)\Big|_- d\boldsymbol{y}\\ &= -\int_{B_\alpha^c} \nabla_y \times \mu_0^{-1}\nabla_y \times \boldsymbol{A}_\alpha \cdot ((\boldsymbol{y}-\boldsymbol{z})_k\boldsymbol{e}_p) d\boldsymbol{y}\\ &\quad + \int_{B_\alpha^c} \mu_0^{-1}\nabla_y \times \boldsymbol{A}_\alpha \cdot (\boldsymbol{e}_k \times \boldsymbol{e}_p) d\boldsymbol{y}\\ &= \int_{B_\alpha^c} \mu_0^{-1}\nabla_y \times \boldsymbol{A}_\alpha \cdot (\boldsymbol{e}_k \times \boldsymbol{e}_p) d\boldsymbol{y} - \int_{B_\alpha^c} \boldsymbol{J}_0 \cdot ((\boldsymbol{y}-\boldsymbol{z})_k\boldsymbol{e}_p) d\boldsymbol{y}\end{aligned}$$

where the first term is skew symmetric. We can rewrite $\boldsymbol{J}_0 = \nabla \times \mu_0^{-1}\nabla \times \boldsymbol{A}_0$ in B_α^c, and noting that $\boldsymbol{A}_0$ satisfies (14) with $\alpha = 0$, we find that

$$\begin{aligned}&\int_{B_\alpha^c} \boldsymbol{J}_0 \cdot ((\boldsymbol{y}-\boldsymbol{z})_k\boldsymbol{e}_p) d\boldsymbol{y}\\ &= \int_{\Gamma_\alpha} \boldsymbol{n}^+ \cdot \left(\mu_0^{-1}\nabla_y \times \boldsymbol{A}_0 \times ((\boldsymbol{y}-\boldsymbol{z})_k\boldsymbol{e}_p)\right) d\boldsymbol{y}\\ &\quad + \int_{B_\alpha^c} \boldsymbol{e}_k \times \boldsymbol{e}_p \cdot \mu_0^{-1}\nabla_y \times \boldsymbol{A}_0 d\boldsymbol{y}\\ &= \int_{B_\alpha} \left(\mu_0^{-1}\nabla_y \times \boldsymbol{A}_0 \cdot \boldsymbol{e}_k \times \boldsymbol{e}_p\right) d\boldsymbol{y}\\ &\quad + \int_{B_\alpha^c} \boldsymbol{e}_k \times \boldsymbol{e}_p \cdot \mu_0^{-1}\nabla_y \times \boldsymbol{A}_0 d\boldsymbol{y}\end{aligned}$$

which is also skew symmetric with respect to k and p. A similar treatment can also be applied for excitation by a uniform field, which shows that I_4 is also skew symmetric with respect to k and p in this case also. Consequently, $\mathcal{Q}$ is a skew symmetric rank 2 tensor and its components satisfy

$$(\mathcal{Q})_{kp} = -(\mathcal{Q})_{pk} = -\frac{1}{2}(\mathcal{Q})_{ms}\epsilon_{kpr}\epsilon_{smr}$$

and so

$$\begin{aligned}\mathrm{I}_2 &= \mathrm{i}\omega\sigma_*\epsilon_{ijp}\left(\boldsymbol{D}_x^2 G(\boldsymbol{x},\boldsymbol{z})\right)_{jk}(\mathcal{Q})_{kp}\\ &= -\frac{\mathrm{i}\omega\sigma_*}{2}\epsilon_{ijp}\epsilon_{kpr}\left(\boldsymbol{D}_x^2 G(\boldsymbol{x},\boldsymbol{z})\right)_{jk}\epsilon_{smr}(\mathcal{Q})_{ms}\\ &= -\frac{\mathrm{i}\omega\sigma_*}{2}(\delta_{ik}\delta_{jr} - \delta_{ir}\delta_{jk})\left(\boldsymbol{D}_x^2 G(\boldsymbol{x},\boldsymbol{z})\right)_{jk}\epsilon_{rms}(\mathcal{Q})_{ms}.\end{aligned}$$

Using the symmetry $(\boldsymbol{D}_x^2 G(\boldsymbol{x},\boldsymbol{z}))_{ri} = (\boldsymbol{D}_x^2 G(\boldsymbol{x},\boldsymbol{z}))_{ir}$ and trace free property $(\boldsymbol{D}_x^2 G(\boldsymbol{x},\boldsymbol{z}))_{kk} = 0$, we find that

$$\mathrm{I}_2 = -\frac{\mathrm{i}\omega\sigma_*}{2}\left(\boldsymbol{D}_x^2 G(\boldsymbol{x},\boldsymbol{z})\right)_{ir}\int_{B_\alpha} ((\boldsymbol{y}-\boldsymbol{z}) \times \boldsymbol{A}_\alpha)_r d\boldsymbol{y}. \tag{53}$$

Finally, using (51) and (53) in (50) gives the expression for $(\boldsymbol{H}_\alpha - \boldsymbol{H}_0)(\boldsymbol{x})_i$ found in (16).

Acknowledgment

The authors would like to thank Prof. Peyton, Prof. Shubitidze, and Dr. Yin for their helpful discussions and comments on polarizability tensors. All data are provided in full in Section V of this paper.

References

[1] O. A. Abdel-Rehim, J. L. Davidson, L. A. Marsh, M. D. O'Toole, and A. J. Peyton, "Magnetic polarizability tensor spectroscopy for low metal anti-personnel mine surrogates," *IEEE Sensors J.*, vol. 16, no. 10, pp. 3775–3783, May 2016.

[2] D. Ambruš, D. Vasić, and V. Bilas, "Robust estimation of metal target shape using time-domain electromagnetic induction data," *IEEE Trans. Instrum. Meas.*, vol. 65, no. 4, pp. 795–807, Apr. 2016.

[3] H. Ammari, T. Boulier, J. Garnier, and H. Wang, "Shape recognition and classification in electro-sensing," *Proc. Nat. Acad. Sci. USA*, vol. 111, no. 32, pp. 11652–11657, 2014.

[4] H. Ammari, J. Chen, Z. Chen, J. Garnier, and D. Volkov, "Target detection and characterization from electromagnetic induction data," *J. Math. Pures Appl.*, vol. 101, no. 1, pp. 54–75, Jan. 2014.

[5] H. Ammari, J. Chen, Z. Chen, D. Volkov, and H. Wang, "Detection and classification from electromagnetic induction data," *J. Comput. Phys.*, vol. 301, pp. 201–217, Nov. 2015.

[6] H. Ammari and H. Kang, *Polarization and Moment Tensors: With Applications to Inverse Problems*. New York, NY, USA: Springer, 2007.

This article has been accepted for inclusion in a future issue of this journal. Content is final as presented, with the exception of pagination.

[7] C. O. Ao, H. Braunisch, K. O'Neill, and J. A. Kong, "Quasi-magnetostatic solution for a conducting and permeable spheroid with arbitrary excitation," *IEEE Trans. Geosci. Remote Sens.*, vol. 40, no. 4, pp. 887–897, Apr. 2002.

[8] B. E. Barrowes, K. O'Neill, T. M. Grzegorczyk, X. Chen, and J. A. Kong, "Broadband analytical magnetoquasistatic electromagnetic induction solution for a conducting and permeable spheroid," *IEEE Trans. Geosci. Remote Sens.*, vol. 42, no. 11, pp. 2479–2489, Nov. 2004.

[9] C. E. Baum, "Low-frequency near-field magnetic scattering from highly, but not perfectly," Univ. New Mexico, Albuquerque, NM, USA, Interaction Notes 499, 1993.

[10] C. E. Baum, "The magnetic polarizability dyadic and point symmetry," Univ. New Mexico, Albuquerque, NM, USA, Interaction Notes 502, 1994.

[11] C. E. Baum, "Discrimination of buried targets via the singularity expansion," Univ. New Mexico, Albuquerque, NM, USA, Interaction Notes 521, 1996.

[12] C. E. Baum, *The Singularity Expansion Method In Electromagnetics: A Summary Survey And Open Questions*. Albuquerque, NM, USA: SUMMA Found., 2012.

[13] A. Bossavit, "Magnetostatic problems in multiply connected regions: Some properties of the curl operator," *IEE Proc. A, Phys. Sci., Meas. Instrum., Manage. Edu.-Rev.*, vol. 135, no. 3, pp. 179–187, Mar. 1988.

[14] H. Braunisch, C. O. Ao, K. O'Neill, and J. A. Kong, "Magnetoquasistatic response of conducting and permeable prolate spheroid under axial excitation," *IEEE Trans. Geosci. Remote Sens.*, vol. 39, no. 12, pp. 2689–2701, Dec. 2001.

[15] Y. Das, J. E. McFee, J. Toews, and G. C. Stuart, "Analysis of an electromagnetic induction detector for real-time location of buried objects," *IEEE Trans. Geosci. Remote Sens.*, vol. 28, no. 3, pp. 278–288, May 1990.

[16] B. Dekdouk, C. Ktistis, L. A. Marsh, D. W. Armitage, and A. J. Peyton, "Towards metal detection and identification for humanitarian demining using magnetic polarizability tensor spectroscopy," *Meas. Sci. Technol.*, vol. 26, no. 11, p. 115501, 2015.

[17] T. M. Gregorcyzk, B. Zhang, J. Kong, B. E. Barrowes, and K. O'Neill, "Electromagnetic induction from highly permeable and conductive ellipsoids under arbitrary excitation: Application to the detection of unexploded ordnances," *IEEE Trans. Geosci. Remote Sens.*, vol. 46, no. 4, pp. 1164–1176, Apr. 2008.

[18] T. M. Grzegorczy, B. E. Barrowes, F. Shubitidze, J. P. Fernández, and K. O'Neill, "Simultaneous identification of multiple unexploded ordnance using electromagnetic induction sensors," *IEEE Trans. Geosci. Remote Sens.*, vol. 49, no. 7, pp. 2507–2517, Jul. 2011.

[19] J. D. Jackson, *Classical Electrodynamics*. Hoboken, NJ, USA: Wiley, 1967.

[20] L. D. Landau and E. M. Lifshitz, *Electrodynamics of Continuous Media*, 1st ed. Oxford, U.K.: Pergammon Press, 1960.

[21] P. D. Ledger and W. R. B. Lionheart, "Characterizing the shape and material properties of hidden targets from magnetic induction data," *IMA J. Appl. Math.*, vol. 80, no. 6, pp. 1776–1798, 2015.

[22] P. D. Ledger and W. R. B. Lionheart, "Understanding the magnetic polarizability tensor," *IEEE Trans. Magn.*, vol. 52, no. 5, May 2016, Art. no. 6201216.

[23] P. D. Ledger and W. R. B. Lionheart, "Generalised magnetic polarizability tensors," *Math. Methods Appl. Sci.*, 2018, doi: 10.1002/mma.4809. [Online]. Available: https://arxiv.org/abs/1705.00580

[24] A. J. Peyton, D. W. Armitage, L. A. Marsh, C. Ktistis, W. R. B. Lionheart, and A. Jarvi, "Walk through metal detection system," U.S. Patent 9 562 986, Feb. 7, 2017.

[25] W. R. B. Lionheart and P. J. Withers, "Diffraction tomography of strain," *Inverse Problems*, vol. 31, no. 4, p. 045005, 2015.

[26] J. Makkonen *et al.*, "KNN classification of metallic targets using the magnetic polarizability tensor," *Meas. Sci. Technol.*, vol. 25, no. 5, p. 055105, 2014.

[27] J. Makkonen *et al.*, "Improving reliability for classification of metallic objects using a WTMD portal," *Meas. Sci. Technol.*, vol. 26, no. 10, p. 105103, 2015.

[28] L. A. Marsh, C. Ktisis, A. Järvi, D. W. Armitage, and A. J. Peyton, "Three-dimensional object location and inversion of the magnetic polarizability tensor at a single frequency using a walk-through metal detector," *Meas. Sci. Technol.*, vol. 24, no. 4, p. 045102, 2013.

[29] L. A. Marsh, C. Ktistis, A. Järvi, D. Armitage, and A. J. Peyton, "Determination of the magnetic polarizability tensor and three dimensional object location for multiple objects using a walk-through metal detector," *Meas. Sci. Technol.*, vol. 25, no. 5, p. 055107, 2014.

[30] S. J. Norton and I. J. Won, "Identification of buried unexploded ordnance from broadband electromagnetic induction data," *IEEE Trans. Geosci. Remote Sens.*, vol. 39, no. 10, pp. 2253–2261, Oct. 2001.

[31] S. J. Norton, W. A. SanFilipo, and I. J. Won, "Eddy-current and current-channeling response to spheroidal anomalies," *IEEE Trans. Geosci. Remote Sens.*, vol. 43, no. 10, pp. 2200–2209, Oct. 2005.

[32] J. A. Osborn, "Demagnetizing factors of the general ellipsoid," *Phys. Rev.*, vol. 67, pp. 351–357, Jun. 1945.

[33] O. A. A. Rehim, J. L. Davidson, L. A. Marsh, M. D. O'Toole, D. W. Armitage, and A. J. Peyton, "Measurement system for determining the magnetic polarizability tensor of small metallic targets," in *Proc. IEEE Sensor Appl. Symp.*, Zadar, Croatia, 2015.

[34] F. Shubitidze, "EMI modeling for UXO detection and discrimination underwater," Dept. Defence Strategic Environ. Res. Develop. Program, Thayer School Eng., Dartmouth College, Tech. Rep. MR-1632, 2011.

[35] F. Shubitidze *et al.*, "Application of the normalized surface magnetic charge model to UXO discrimination in cases with overlapping signals," *J. Appl. Geophys.*, vol. 61, pp. 292–303, Mar. 2007.

[36] F. Shubitidze, K. O'Neill, S. A. Haider, K. Sun, and K. D. Paulsen, "Application of the method of auxiliary sources to the wide-band electromagnetic induction problem," *IEEE Trans. Geosci. Remote Sens.*, vol. 40, no. 4, pp. 928–942, Apr. 2002.

[37] F. Shubitidze, K. O'Neill, K. Sun, and K. D. Paulsen, "Investigation of broadband electromagnetic induction scattering by highly conductive, permeable, arbitrarily shaped 3-D objects," *IEEE Trans. Geosci. Remote Sens.*, vol. 42, no. 3, pp. 540–556, Mar. 2004.

[38] W. R. Smythe, *Static and Dynamic Electricity*. New York, NY, USA: McGraw-Hill, 1968.

[39] J. Stratton, *Electromagnetic Theory*. New York, NY, USA: McGraw-Hill, 1941.

[40] J. R. Wait, "A conducting sphere in a time varying magnetic field," *Geophysics*, vol. 16, no. 4, pp. 666–672, 1951.

[41] J. R. Wait, "A conducting permeable sphere in the presence of a coil carrying an oscillating current," *Can. J. Phys.*, vol. 31, no. 4, pp. 670–678, 1953.

[42] J. R. Wait, "On the electromagnetic response of a conducting sphere to a dipole field," *Geophysics*, vol. 25, no. 3, pp. 649–658, 1960.

[43] J. R. Wait and K. P. Spies, "Quasi-static transient response of a conducting permeable sphere," *Geophysics*, vol. 34, no. 5, pp. 789–792, 1969.

[44] Y. Zhao, W. Yin, C. Ktistis, D. Butterworth, and A. J. Peyton, "On the low-frequency electromagnetic responses of in-line metal detectors to metal contaminants," *IEEE Trans. Instrum. Meas.*, vol. 63, no. 12, pp. 3181–3189, Dec. 2014

[45] Y. Zhao, W. Yin, C. Ktistis, D. Butterworth, and A. J. Peyton, "Determining the electromagnetic polarizability tensors of metal objects during in-line scanning," *IEEE Trans. Instrum. Meas.*, vol. 65, no. 5, pp. 1172–1181, May 2016.

Paul D. Ledger received the B.Eng. degree in civil engineering with specialization in computational mechanics from the University of Birmingham, Birmingham, U.K., in 1998, and the M.Sc. degree in computational modeling and finite elements with specialization in engineering mechanics and Ph.D. degree in *hp*-finite elements for electromagnetic scattering from Swansea University, Swansea, U.K., in 1999 and 2002, respectively.

He is currently an Associate Professor with the College of Engineering, Swansea University Bay Campus. His research interests include high-order/*hp*-finite elements applied to problems in computational electromagnetism, error estimation and adaptivity, and the computational solution of coupled and inverse problems.

William R. B. Lionheart received the B.Sc. degree in applied mathematics from The University of Warwick, Coventry, U.K., in 1980, and the Ph.D. degree in electrical impedance tomography from Oxford Brookes University, Oxford, U.K.

He is currently a Professor of applied mathematics with The University of Manchester, Manchester, U.K., where he was involved in a wide range of inverse problems in medicine and industry, including electrical impedance tomography, magnetic induction tomography, x-ray computed tomography, and position emission tomography. His interest in low-frequency electromagnetic imaging led to his involvement in the civilian land mine clearance charity—Find a Better Way—in which he was involved in founding.

Prof. Lionheart was a recipient of the Royal Society's 2015 Wolfson Research Merit Award for "Novel Methods in Tomography Imaging: Rich Tomography and Fast Dynamic Imaging."